Response to Reviews

We thank the two reviewers for their constructive comments to improve the manuscript. Their comments are reproduced below with our responses in blue.

Reviewer #1

This paper proposed a machine learning method to predict gridded monthly wildfire burned area during 2002-2015 over the South Central United States and identify the relative importance of the predicted factors on the burned area for both the winter-spring and summer fire seasons. The method is able to alleviate the problem of unevenly-distributed burned area data due to the grid-level resolution. The result is interesting and constructive to some extent. The authors said the machine learning method can achieve the R2 value of ~0.4. However, this result is hard to say it as a high accuracy. The authors can consider to compare more machine learning algorithms, such as AdaBoost, XGBoost. The low accuracy will also affect the reliability of the importance of predicted factors. Therefore, I would recommend a major revision.

We appreciate the feedback from the reviewer. It is easily understood that the prediction accuracy of wildfire burned areas will increase as the spatial and temporal resolution of the prediction model decreases. In comparison to previous studies that predict wildfire burned areas, our work is unique in two aspects: (1) our prediction performance (R^2 of ~0.4) was reported at the 0.5° x 0.5°-grid scale rather than over an aggregated spatial domain; (2) we did not exclude unburned grids or small burned grids from the prediction. Since very few published studies had both of these two features, we can only compare our results with the prior studies predicting burned area at similar spatial scales as our work (see the Table R1 below). These studies have R^2 values all below 0.3, despite using a coarser spatial resolution (~100 km x 100 km) and sometimes also a coarser temporal resolution (annually). Considering the complexity of wildfires and intrinsic nature of unevenly distributed burned area, we argue that R^2 value of around 0.4 from our work is a significant improvement over those previously published studies. Furthermore, the machine learning approaches developed by our work were motivated by the need to reduce the uneven distribution of burned area data so as to achieve a higher prediction accuracy.

We tested other boosting methods as suggested by the reviewer and they did not achieve significantly better results (see our response to comment #11). In addition, at this stage we do not foresee physical explanations to adopt these boosting methods. To address the reviewer's concern, we have rewritten the comparison of our work with others in the revised manuscript and elaborated in more detail how much better our model is compared with previously published works.

Table R1. Studies using statistical methods to estimate burned area at spatial scales similar as this study

Region	**period**	**Method**	**Spatial scale**	**Temporal scale**	**R^2**	**References**
Spain	1990-2008	MARS	25 km x 25 km ~100 km x 100 km	Monthly	Median correlation R=0.29 (R^2~0.08)	Bedia et al. (2014)
EU-Mediterranean	1985-2011	MLR	~108 km x 108 km	Annual	Median R^2=0.28	Urbieta et al. (2015)
Pacific western coast of USA	1985-2011	MLR	~108 km x 108 km	Annual	Median R^2=0.22	Urbieta et al. (2015)

More detailed discussion is presented below in the specific comment #11.

Regarding the reliability of the inferred importance of predicted factors, our results are robust based on the optimized model with the best results and the given set of predictor variables. To verify this, we also conducted 50 times 10-fold cross-validation by randomizing the order of all the data each time. The ranks of the variables by the median values of %IncMSE are identical to the ranks of the variables in our initial results. This indicates that feature importance identified by the random forest model is reliable and stable. We have included the above discussions in the revised manuscript.

1. P1L25: have been seen increasing?

We have changed the sentence to "many regions of the world have experienced an increase in frequency and intensity of wildfires …" (line 27).

2. P2L51: You said the machine learning methods were used to estimate total burned area aggregated over a large-scale domain in past studies. In this study, you focus on the grid-level resolution. Could you describe what the resolution of past studies is? Do these works have the issue of the unbalanced distributed burned area?

The resolution of past studies ranges from 25 km x 25 km to 2000 km x 2000 km, as listed in Table S1. The spatial resolution of the phytoclimatic zones in Bedia et al. (2014) ranges from 25 km x 25 km to 100 km x 100 km; the European countries in Amatulli et al. (2013) had the scales ranging from 300 km x 300 km to 1000 km x 1000 km. We have added the spatial and temporal resolution of these two studies mentioned in the main text (line 50-54).

For these studies, depending on the spatial scale, temporal scale, and wildfire characteristics (fire frequency, intensity etc.), the burned area distribution can be normal-distributed or right-skewed. Generally, studies predicting annual burned area

on a country scale (spatial scale larger than 100 km x 100 km) do not have the issue of uneven-distributed burned area because the burned area are already aggregated. For example, Amatulli et al. (2013) shows the distributions of annual burned area for the countries in European Mediterranean (spatial scales ranging from 300 km x 300 km to 1000 km x 1000 km). For most of the countries, the burned area is normally distributed (Fig R1 below).

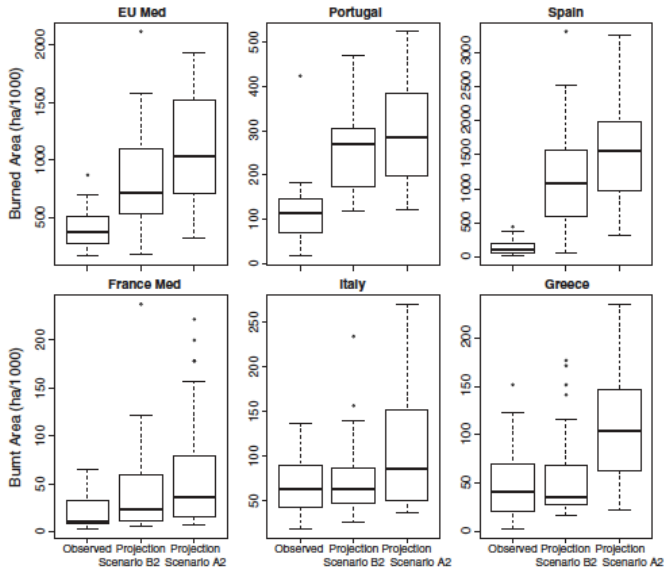

Fig. R1. Box plots of annual observed (left) and projected burned area in all study regions using the MARS models under B2 (middle) and A2 scenarios (right) for the European countries (adopted from Amatulli et al (2013); Fig. 8).

Another example of Carvalho et al. (2008) demonstrates that the distribution of burned area varies by districts in Portugal (spatial scales ranging from 25 km x 25 km to 100 km x 100 km). As Fig. R2 shows, the annual burned area distribution can be like a normal distribution for districts such as Braganca, or it can be very right-skewed for districts such as Evora and Portalegre. We also included the above example and associated discussions in the revised manuscript in line 322-325.

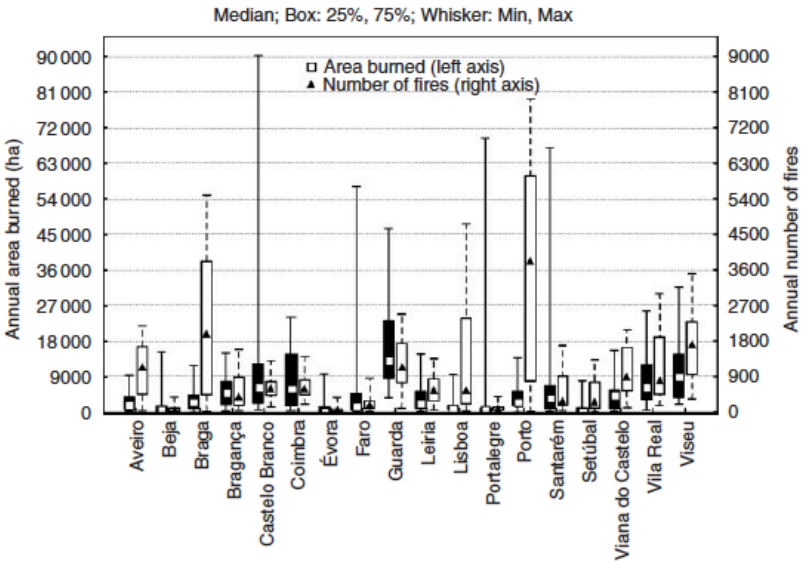

Fig. R2. Box plots of annual burned area and number of fires by Portuguese district for 1980-2004 period (adopted from Carvalho et al. (2008); Fig. 3b).

3. P3L83: The small fire is less than 10 ha, and the large fire is greater than 100 ha. However, the small fire is defined as less than 25 ha, and the large fire is greater than 150 ha in P2L58. Could you explain why they are different?

The definition of small fires at 25 ha and large fires at 150 ha was based on Steel et al. (2015) while the criterion of 10 ha was according to Yue et al. (2013). To avoid confusion and ensure the consistency, we changed the definition in line 183-186 from "10 ha" to "25 ha" and "100 ha" to "150 ha" and updated the statistics.

4. I don't think Figure 2 looks nice and it should be re-organized better. For example, the arrow between step 1 and step 2 confuses that there may be an input-output relationship. In fact, is it correct that they are independent processes?

We agree with the reviewer's concern and suggestions. We have re-organized and updated Figure 2, as shown below. Step 1 includes a quantile regression forest and step 2 includes a logistic regression with the same set of input variables. These two steps are independent processes but they are followed the order of the listed steps.

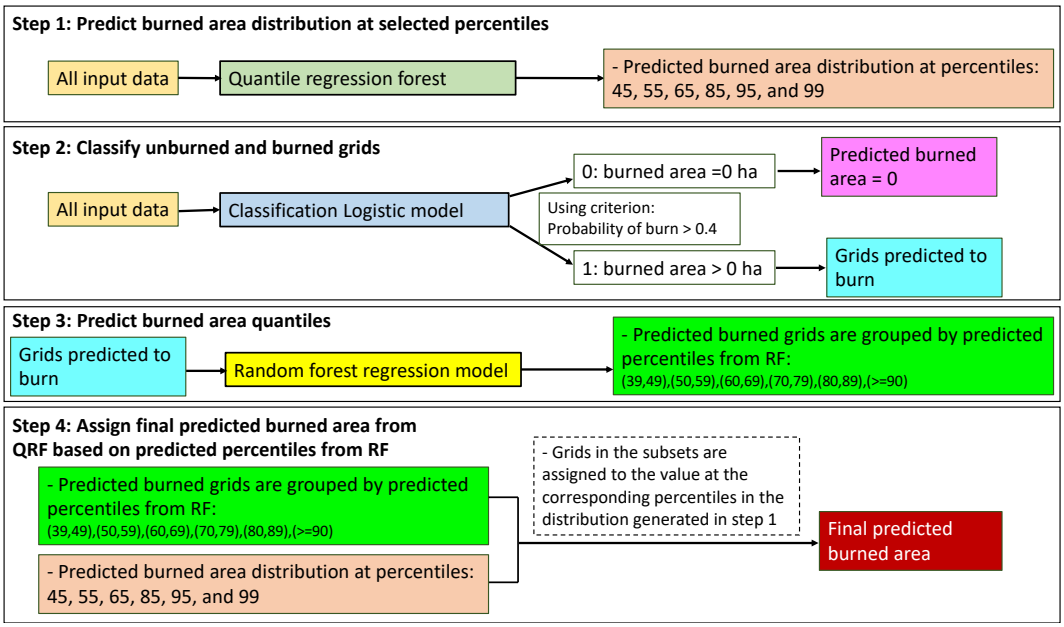

Fig. R3. Illustration of the steps in the developed model. The model includes four steps and three machine learning algorithms, including a logistic model (dark blue) classifying a grid with non-zero burned area or not, a random forest model (yellow) predicting quantiles of burned area, and a quantile regression forest (dark green) predicting conditional burned area distributions. (This figure is now Fig. 2. In the revised manuscript)

5. P3L90: The description of the four steps is not very clear. This paragraph should be rewritten. Is it correct the quantiles are the x-axis of frequency histogram? Why do you choose these quantiles? Will the pre-defined parameters induce uncertainties?

(1) Yes, the quantiles represent to the position of the predicted burned area in the cumulative distribution of all the burned area data. For example, Fig. R4 shows the empirical cumulative distribution functions of the burned area in the winter-spring fire season. The value of quantile at 0.7 can be determined by the value on the x axis, which is 3.74 (log of hectares). To better clarify the idea of quantiles, we have replaced 'quantile' with 'percentile' in the manuscript and rewrote the definition of percentile in line 192-194.

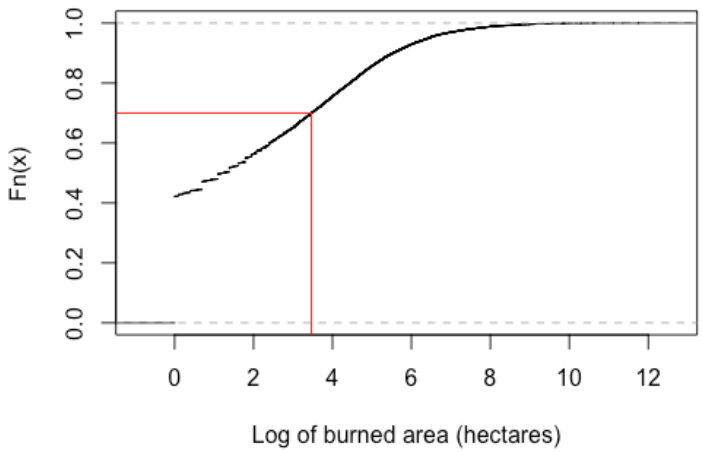

Fig. R4. The empirical cumulative distribution functions of the burned area in the winter-spring fire season. The x axis is the log of burned area and the y axis is the cumulative probability. The red lines here point the value of burned area at quantile 0.7.

(2) The quantiles were chosen to include the whole conditional distribution. The first three quantiles were selected to represent the median values between the lower and upper bounds for the first three subgroups in step 3. The last three quantiles (0.85, 0.95, and 0.99) were chosen based on the assumption that grids with larger predicted burned areas (predicted quantiles > 0.70) in the testing set will have burned area distributions that are more right-shifted than the distribution of the whole training set (Fig. R5). The quantiles were selected to reduce the model bias at the high end of burned areas. We have edited and added the above-mentioned explanations and Fig. R5 into the manuscript in line 199-205. In the revised manuscript, we have replaced 'quantile' with 'percentile'.

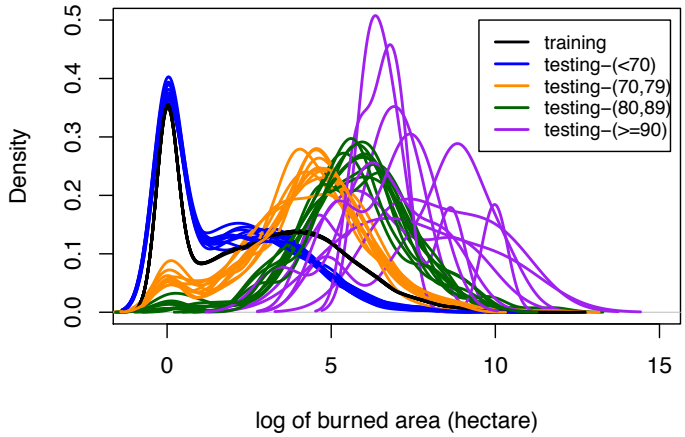

Fig. R5. Probability distribution of burned area for 10 folds of the training set (black line), testing set predicted to have percentiles less than 70 (blue), between 70 and 79 (yellow), between 80 and 89 (green), and equal to or larger than 90 (purple). (This figure is now Fig. S3. in the revised manuscript)

(3) To test the uncertainties that may be introduced by the pre-defined parameters (i.e. quantiles and subgroups), we switched the pre-defined quantiles but fixed the subgroups in the first sensitivity experiment. In this experiment, the last three quantiles were changed to the median values between a new set of lower and upper bounds, (0.75, 0.85, 0.95). As the Table R2 shows, the change of the quantiles has little effect on the overall MAE but affects the prediction of large burned areas with a smaller standard deviation in predicted values and larger MAE. Then we designed the second experiment by changing the number of subgroups, their ranges, and the corresponding quantiles. Changing both subgroups and quantiles has a marginal impact on MAE, although the standard deviation of the prediction is smaller than the results with the chosen quantiles and subgroups.

Generally, changing pre-defined parameters has little effect on overall MAE for the two fire seasons but the MAE of large burned area is larger and standard deviation of the predicted values becomes smaller. The pre-defined parameters may lead to uncertainties mostly affect the spread of the predictions and the magnitudes of large burned areas. Despite the sensitivities, the prediction model with the chosen quantiles is able to predict burned area at 0.5° x 0.5°-grid scale and achieve higher prediction accuracy compared to prior studies. Table R2 and the above discussions have been included into the manuscript (line 528-537).

Table R2. Comparison of MAE, MAE of large burned area, and standard deviation of predictions between the model with the chosen quantiles, quantile test 1, and quantile test set2 (This table is now Table S7 in the revised manuscript)

Model	**With the chosen quantiles***	**Quantile test set 1***	**Quantile test set 2***
MAE (log of area; winter-spring)	1.37	1.30	1.29
MAE of large burned area† (log of area; winter-spring)	2.13	2.64	2.81
Standard deviation of predictions (log of area; winter-spring)	2.42	2.09	2.09
MAE (log of area; summer)	1.17	1.12	1.11
MAE of large burned area† (log of area; summer)	2.25	2.42	2.52
Standard deviation of predictions (log of area; summer)	2.19	1.93	1.92

* Model developed in this study: Use the selected quantiles of 0.45, 0.55, 0.65, 0.85, 0.95, and 0.99 and six subgroups of (0.39, 0.49), (0.50, 0.59), (0.60, 0.69), (0.70, 0.79), (0.80, 0.89), (>=0.90).
* Set 1: Use the selected quantiles of 0.45, 0.55, 0.65, 0.75, 0.85, and 0.95 and six subgroups of (0.39, 0.49), (0.50, 0.59), (0.60, 0.69), (0.70, 0.79), (0.80, 0.89), (>=0.90).

* Set 2: Use the selected quantiles of 0.475, 0.63, 0.78, and 0.93 and four subgroups of (0.39, 0.55), (0.56, 0.70), (0.71, 0.85), (0.86, 1.00).

† Large burned area here is defined as the burned area larger than 90th percentile.

6. P3L90: Although the authors claim that the four steps method will alleviate the problem of uneven-distributed dataset, the multi-steps will introduce some risks. For example, if the second step wrongly classifies the burned area as the nonburned area, the bias will be amplified because it won't enter into step 3.

The reviewer is correct that biases from one step could be propagated to the subsequent steps, for example when the burned grids are predicted not to burn or when the unburned grids are predicted to burn. For the first case, when the burned grids are incorrectly predicted not to burn, the low bias is introduced because the burned grids would not proceed to step 3. For the second case, inclusion of unburned grids in step 3 may introduce a positive bias. We have included the discussions of the error propagation in section 6 (line 511-513).

To demonstrate our four-step model can achieve a higher accuracy and alleviate the issue of uneven-distributed dataset, we compare the prediction performance using random forest alone with that of the four-step model developed in this study, as shown in the Table R3 below:

Table R3. Comparison of MAE and skewness between the RF model and the developed model (The information of this table is now included into the Table S2 in the revised manuscript)

Model	**RF alone**	**Model developed in this study**
MAE (winter-spring)	1.34	1.13
Skewness (winter-spring)	37.40 (burned area)	0.70 (quantiles)
MAE (summer)	0.70	0.57
Skewness (summer)	33.83 (burned area)	0.96 (quantiles)

Skewness is a measure of the asymmetry of the probability distribution of a random variable about its mean. The skewness of a random variable X is the third standardized moment $\widetilde{\mu_3}$, defined as:

$$\widetilde{\mu_3} = E\left[\left(\frac{X-\mu}{\sigma}\right)^3\right] = \frac{\mu_3}{\sigma^3} = \frac{E[(X-\mu)^3]}{(E[(X-\mu)^2])^{3/2}} = \frac{\kappa_3}{\kappa_2^{3/2}}$$

where μ is the mean, σ is the standard deviation, E is the expectation operator, μ_3 is the third central moment, and κ_t are the t-th cumulants. If skewness is less than -1 or greater than +1, the distribution is highly skewed. If skewness is between -1 and -0.5 or between +0.5 and +1, the distribution is moderately skewed. If skewness is between -0.5 and 0.5, the distribution is approximately symmetric. The positive value indicates that the tail is on the right side of the distribution while negative value indicates that the tail is on the left.

Our model has a lower MAE, by 15% and 19% for the winter-spring and summer fire season, respectively, compared to the single RF model. The distribution of the quantiles in the developed model is more uniform than the distribution of the burned area, as shown in Figure R6 below and the skewness. We have added a discussion of this issue in the text (line 355-365) and included Table R3 in the supplementary information. The information of skewness calculation has been included in the supplementary information. Note that we have replaced 'quantile' with 'percentile' in the manuscript to better clarify the idea of quantiles.

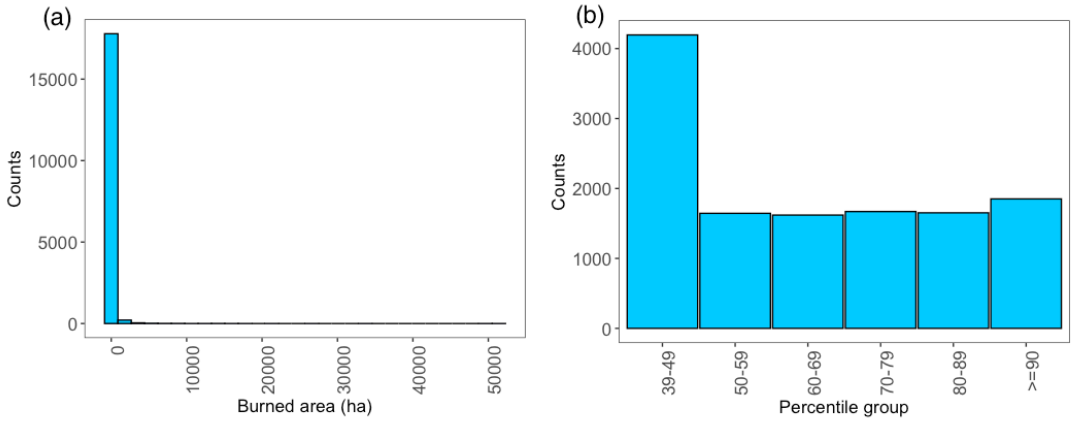

Fig. R6. (a) Histogram of burned area (b) Histogram of the percentile groups of burned area for the winter-spring fire season. (This figure is now Fig. S2. In the revised manuscript)

7. P4L126: Please explain the assumption or give the reference that grids with larger burned area will have more right-shifted burned area distribution than the distributions of the training set.

The above-mentioned Figure R5 shows the burned area distributions of training sets and testing sets categorized by predicted quantile groups. Grids that are predicted to have larger burned area (predicted quantiles larger than 0.70) have more right-shifted burned area distributions compared to the distribution of the training set. We have included the figure and explained the assumption in the manuscript (line 199-205 and Fig S3).

8. P6L171: Please add references.

We have added references in line 106-108.

9. P8L223: Please add the F1-score performance criteria because you mentioned it in L235.

We have added the description of F1-score in line 267-270.

10. P8L235: Could you please plot the AUC curve so that it could help to analyze the TP rate and FP rate. You can also analyze the F1-score performance by Precision

and Recall. This will help to understand whether the classifier is underprediction or overprediction.

The ROC curves are included in the supplementary (Fig S4), as demonstrated below.

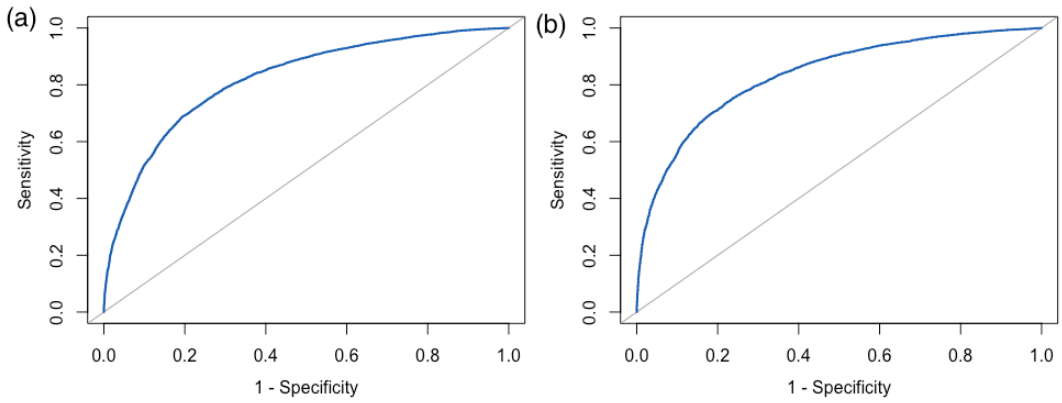

Fig. R7. The ROC curve of burning classification for the (a) winter-spring and (b) summer fire season. (This figure is now Fig. S4. In the revised manuscript)

The ROC curves show good performance of the models, given that the ROC curves are toward the upper left corner and the AUC for the two fire seasons are 0.82 and 0.83. The accuracy and F1-score are 0.74 and 0.79 for the winter-spring fire season. For the summer fire season, the accuracy and F1-score are 0.74 and 0.77. The above results demonstrate the model ability of predicting burned grids with the optimal balance of recall and precision. The values of AUC, recall, precision, and F1-score are also updated in Table 2. We have included the results and discussions of model performance in the main text (line 292-298).

11. P8L235: The performance accuracy of the classifier and the regressor in Table 2 is not very high. Typically, the F1-score of a good classifier can achieve over 0.8 and the RMSE of a good regressor is lower than 0.2. Could you compare your results with some other machine learning methods, such as Adaboost, XGBoost.

We compared our classification model results with some other machine learning methods (the parameters of each model have been optimized):

Table R4. Comparison of accuracy, recall, precision, and F1-score between the logistic regression model, RF model and XGBoost model

Model	**Logistic regression (model for this study)**	**Random forest**	**XGBoost**
Winter-spring fire season			
Accuracy	0.74	0.82	0.80
Recall	0.88	0.86	0.86
Precision	0.73	0.83	0.80
F1-score	0.79	0.84	0.83
Summer fire season			
Accuracy	0.74	0.81	0.81
Recall	0.84	0.82	0.82
Precision	0.71	0.82	0.81
F1-score	0.77	0.82	0.81

RF and XGboost show better performance in terms of accuracy, precision, and F1-score. However, they identify less burned grids (value of Recall) and require more parameter tuning and runtime, compared to logistic model. Considering the comparable performance, more identified burned grids, less model tuning, and less runtime, we chose logistic model as our classification model because it can be simply applied to different regions which is a competitive advantage for future applications of the prediction model.

As for the burned area prediction, we've compared our results with RF model in question 6. Here we included the model results from XGBoost, as it shows below:

Table R5. Comparison of MAE and skewness between the developed model, RF model, XGBoost model (This table is now Table S2 in the revised manuscript)

Metrics	**Model developed in this study**	**RF alone**	**XGBoost alone**
MAE (winter-spring)	1.13	1.34	1.26
Skewness (winter-spring)	0.70 (quantiles)	37.40 (burned area)	37.40 (burned area)
MAE (summer)	0.57	0.70	0.67
Skewness (summer)	0.96 (quantiles)	33.83 (burned area)	33.83 (burned area)

Our four-step model has a lower MAE, which deceases by 11% and 15% for the winter-spring and summer fire season, respectively, compared to the XGboost model. The

developed model shows better performance in predicting burned area, compared to using RF or XGboost model. The model results from XGboost were also included in the Table S2 and corresponding discussion in the manuscript (line 355-365).

12. What does "630" mean in Table 2?
We have removed the misplaced line number 630 from Table 2.

13. P8L247: Please add some references for past studies.
The comparison of model performance to the previous studies has been rewritten and the associated references can be found in the manuscript (line 299-330).

14. P8L251: You compare your results with Chen et al. (2016) and Liu and Wimberly (2015). I wonder whether they are comparable if they are under different factors, different periods and different regions.
Since there are very few studies predicting gridded burned area directly and among them there is no study focusing on the South Central US, we chose to compare our results with these studies in terms of the approaches (i.e. excluding unburn grids or not), the temporal and spatial resolution, and the percent of variance explained by the model (i.e. R-square), regardless of their study regions, periods, and used predictors.

Although the study regions, study period, and the used predictors in this study are different from prior studies mentioned for comparison in the main text, the developed model in this study demonstrates some advantages compared to other models. First, both Chen et al. (2016) and Liu and Wimberly (2015) excluded unburned or small-burned grids when building their models, thus failing to capture the response of small fires size to predictor variables. Second, both studies focused on annual burned area in a spatial resolution of 1°x 1°, while the spatial and temporal resolution of our four-step model is finer both spatially and temporally (0.5° x 0.5° and monthly burned area). Our four-step model is able to resolve the fire-predictor relationship in a seasonal and a relatively-finer spatial scale.

We also included other studies with a similar spatial resolution for comparison. Urbieta et al. (2015) used multiple linear regression (MLR) to predict annual burned area of provinces and national forests in the southern countries of the European Union (EUMED) and Pacific Western US (PWUSA) (spatial resolution ~ 108 km x 108 km). For all the provinces/national forests, the median R^2 is 0.28 for EUMED and 0.22 for PWUSA. Carvalho et al. (2008) utilized MLR to predict monthly burned area of Portuguese districts (spatial resolution ranging from 25 km x 25 km to 100 km x 100 km) and their R^2 range from 0.43 to 0.80. Even though they achieved a better model performance for some districts, their models had poorer performance for the districts with very right-skewed burned area distribution (Figure R2 shown above), including Evora (R^2=0.43), Portalegre (R^2=0.45). Another example of Bedia et al. (2014) predicted monthly burned area of phytoclimatic zones in Spain (~ 25 km x 25 km to

100 km to 100 km) by using multivariate adaptive regression splines (MARS) and they obtained R^2 ranging from 0.01 to 0.37.

Although the model performance may vary depending on regions, fire characteristics, time scales, and predictors, the R^2 value of around 0.4 that we achieved to predict monthly burned area at a spatial resolution of 0.5^ox0.5^o is a significant improvement over previously published studies for burned area prediction at such spatiotemporal scale and the improvement was resulted from our efforts to alleviate the issue of unevenly-distributed burned area. We have rewritten the paragraphs to better explain the comparisons and the advantages of our models in line 299-330.

15. Please explain the meaning of the blue line in Figure 3.
The blue line is a best fit to the data by linear regression. We have added the descriptions of the blue line in the caption of Figure 3.

16. P9L281: Although the importance of Random Forest help to identify some key factors, they depend on the accuracy of the machine learning method. If the accuracy is not very high, it will reduce the reliability of the information. On the other hand, the importance can't provide how the change trend of factors affect the prediction.
(1) Based on the optimized model with the best results and the given set of predictor variables, the variable importance of predictors is reliable. Besides model accuracy, stability of the variable importance should also be considered (Han et al., 2012; He and Yu, 2010). To further ensure the variable ranking is stable, we conducted 50 times 10-fold cross-validation by randomizing the order of all the data each time. Figure R8 below shows the distributions of %IncMSE of each variable ranked by the median %IncMSE. Even though the feature importance varies a lot in different runs, the ranks by median values are identical to the variable ranks in our initial results, indicating the feature importance identified by the random forest model is stable. We have included the above discussions in the revised manuscript (line 382-385).

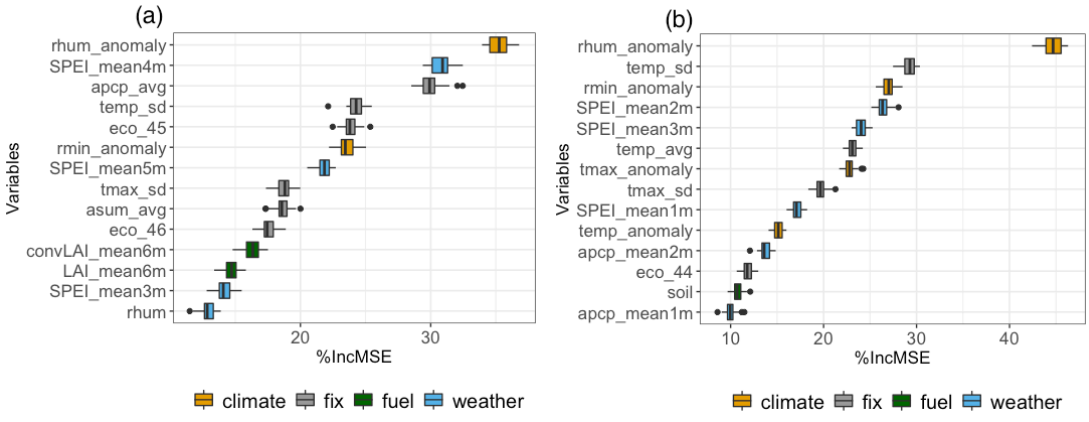

Fig. R8. Box plots of variable importance in %IncMSE from the 50 times 10-fold cross validation for (a) winter-spring and (b) summer fire season. (This figure is now Fig. S6. In the revised manuscript)

(2) Although the variable importance by RF cannot directly provide how the change trend of factors affect the prediction, like the coefficient in the linear regression, the partial dependence plots can be applied to the built model and show the marginal effect of a variable on the prediction performance (Friedman, 2001). The partial dependence plots consider a partial dependence function that is estimated by calculating averages in the training data and can be expressed as:

$$\widehat{f_{xS}}(xS) = \frac{1}{n}\sum_{i=1}^{n}\hat{f}(xS, x_C^{(i)}),$$

where xS is the feature we are interested in and $x_C^{(i)}$ are actual feature values for the features in which we are not interested. This partial function provides the average marginal effect on the prediction for given values of feature S.

Here we provide partial dependence plots for the burned area model and RH anomaly and mean SPEI of the preceding 4 months (the top two variables) for the winter-spring fire season (Fig. R9). For these two variables, there is a significant drop of fitted burned area when RH anomaly is larger than -1 and mean SPEI of the preceding 4 months larger than -0.6. The partial dependence plots demonstrate how change of a variable affects the predicted burned area. We have included the information and the above-mentioned examples in the revised manuscript (line 405-410).

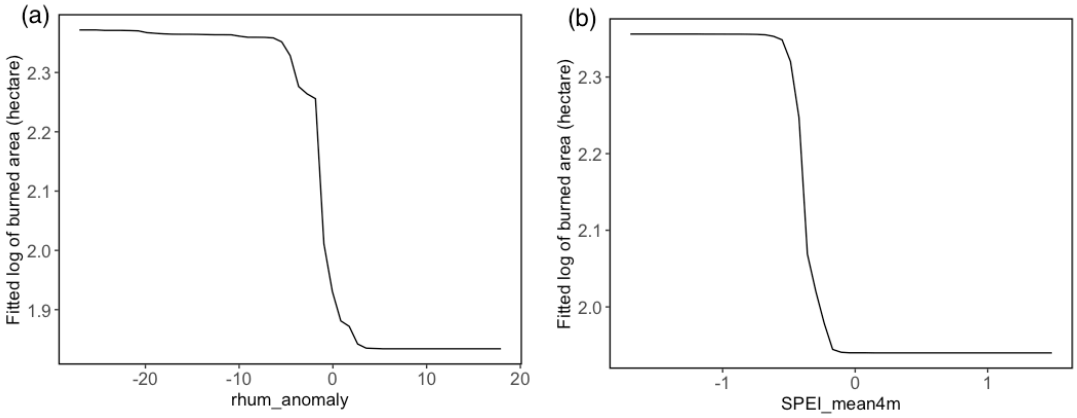

Fig. R9. Partial dependence plots for the burned area model and (a) RH anomaly and (b) mean SPEI of the preceding 4 months for the winter-spring fire season. (This figure is now Fig. S7. In the revised manuscript)

17. P9L299: I can't find the reference "Westerling and Bryant (2008)" in the reference list.
We have included the reference "Westerling and Bryant (2008)" into the reference list.
18. There are several obvious typos in the manuscript, and the English language is poor. I think the authors should be asked to have the manuscript proofread by a native English speaker before the article can be considered for publication in a scientific journal.
We have revised the manuscript and the manuscript has been proofread by a native English speaker.

References:

Amatulli, G., Camia, A. and San-Miguel-Ayanz, J.: Estimating future burned areas under changing climate in the EU-Mediterranean countries, Science of The Total Environment, 450–451, 209–222, doi:10.1016/j.scitotenv.2013.02.014, 2013.

Bedia, J., Herrera, S. and Gutiérrez, J. M.: Assessing the predictability of fire occurrence and area burned across phytoclimatic regions in Spain, Natural Hazards and Earth System Sciences, 14(1), 53–66, doi:https://doi.org/10.5194/nhess-14-53-2014, 2014.

Carvalho, Flannigan, M., Logan, Miranda, A. and Borrego, C.: Fire activity in Portugal and its relationship to weather and the Canadian Fire Weather Index System, International Journal of Wildland Fire, 17, 328–338, doi:10.1071/WF07014, 2008.

Chen, Y., Morton, D. C., Andela, N., Giglio, L. and Randerson, J. T.: How much global burned area can be forecast on seasonal time scales using sea surface temperatures?, Environ. Res. Lett., 11(4), 045001, doi:10.1088/1748-9326/11/4/045001, 2016.

Friedman, J. H.: Greedy Function Approximation: A Gradient Boosting Machine, The Annals of Statistics, 29(5), 1189–1232, 2001.

Han, J., Kamber, M. and Pei, J.: Data Mining: concepts and techniques, Morgan Kaufmann., 2012.

He, Z. and Yu, W.: Stable feature selection for biomarker discovery, Comput Biol Chem, 34(4), 215–225, doi:10.1016/j.compbiolchem.2010.07.002, 2010.

Liu, Z. and Wimberly, M. C.: Climatic and Landscape Influences on Fire Regimes from 1984 to 2010 in the Western United States, PLOS ONE, 10(10), e0140839, doi:10.1371/journal.pone.0140839, 2015.

Steel, Z. L., Safford, H. D. and Viers, J. H.: The fire frequency-severity relationship and the legacy of fire suppression in California forests, Ecosphere, 6(1), 1–23, doi:10.1890/ES14-00224.1, 2015.

Urbieta, I. R., Zavala, G., Bedia, J., Gutierrez, J. M., San Miguel-Ayanz, J., Camia, A., Keeley, J. E. and Moreno, J. M.: Fire activity as a function of fire–weather seasonal severity and antecedent climate across spatial scales in southern Europe and Pacific western USA, Environmental Research Letters, 10(11), doi:10.1088/1748-9326/10/11/114013, 2015.

Yue, X., Mickley, L. J., Logan, J. A. and Kaplan, J. O.: Ensemble projections of wildfire activity and carbonaceous aerosol concentrations over the western United States in the mid-21st century, Atmos Environ (1994), 77, 767–780, doi:10.1016/j.atmosenv.2013.06.003, 2013.

Reviewer #2

Summary: This manuscript described a method for estimating burned area in the southern central region of the United States using three machine learning methods applied serially, with training derived from an existing dataset. The results show some skill in modeling total burned area over large areas. The work is focused mainly on the role of climatic variables in estimating burned area totals. While the methods in this paper might be of interest to the broader community, the manuscript is not well written (the structure is difficult to follow and it requires significant language editing throughout), the results cannot be reproduced because there is not enough information about the input variable processing, and the significance and limitations of the study are not explained well. Again, this method could prove to be useful to the broader community, but the manuscript needs significant work and for that reason I recommend rejecting this paper.

General Comments: While I think the methods presented in the manuscript have potential to produce useful results, the manuscript needs to be improved in order to create a more logical flow of information, better describe the data used, illustrate the output, provide a more complete literature review, and provide details about the usefulness and limitations of this study. Furthermore, it requires editing beyond the scope of scientific peer-review.

We thank the reviewer's comment. We have adjusted the sections of the manuscript to help readers better follow the article, and added more information about data, such as data source and the regridding method. With regards to the literature review, the focus of this study is on machine-learning-based prediction of wildfires and the relative importance of environmental controls of wildfires. Therefore, the literature review was mainly focused on this aspect. To follow the suggestions of the reviewer, we have added more literatures into the revised manuscript, including the ones mentioned by the reviewers. The details of the expected impact (line 70-73 and 558-567) and the limitation of this study (line 510-537) have been included in the manuscript.

(1)

The goals of this study are unclear – is the goal to predict wildfires in the future based on weather conditions, to support climate projections, or to simply estimate the amount of burned area?

The goal of this study is to develop a wildfire burned area prediction model that can be used to quantitatively estimate the contribution of different environmental factors that control wildfires at the grid level. We have stressed the goal of this study in line 69-73. To better represent this goal, we slightly revised the paper title to: "Quantifying the effects of environmental factors on wildfire burned area in South Central US using integrated machine learning techniques"

(2)

A related critique is that the structure of the paper makes it difficult for the reader to follow, there are effectively two methods sections with the results of the first set of methods in the middle.

As suggested, we have moved the validation method (original section 3.1) to Model section (new section 3.2).

(3)

Additionally, the authors never present a figure showing the modeled burned area, which should be the main output of this work and really needs to be emphasized in the main body of the manuscript.

We have moved the original Fig. S1 to the manuscript as Fig. 4 (Fig. R10 below). Fig. R10 shows the maps of monthly mean observed and predicted burned area averaged from 2002-2015 for both fire seasons. In addition to Fig. R10, Fig. 3 and Fig. 5 in the manuscript show the modeled burned area verses the observed burned area at the grid level and at the large-domain level. These results demonstrate that the model has the certain ability in predicting burned area at the grid-scale and at large-domain scale. We have rewritten and reorganized the corresponding paragraphs to emphasize the results in section 4.

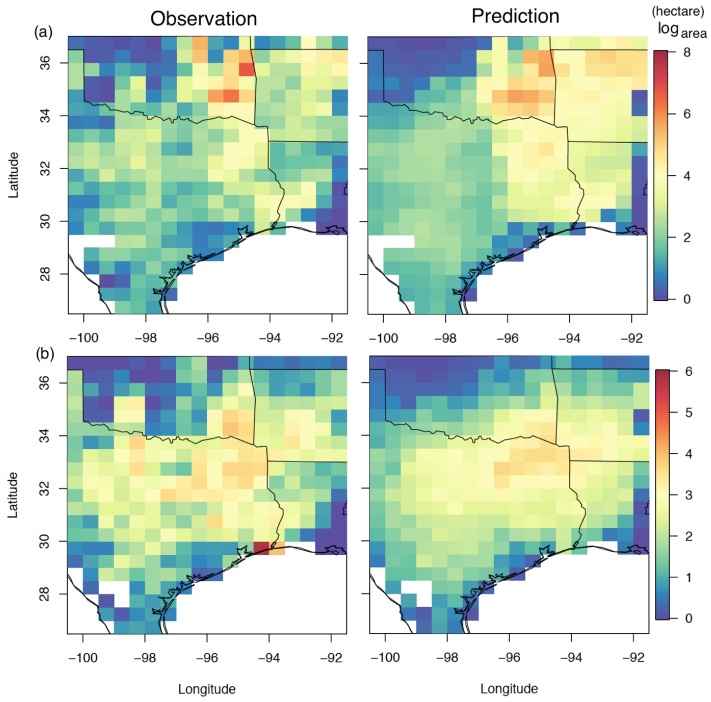

Fig. R10. Map of monthly mean observed and predicted burned area averaged from 2002 to 2015 for the (a) winter-spring and (b) summer fire season. (This figure is now Fig. 4. In the revised manuscript)

(4)

The authors have not considered a large body of wildfire research regarding satellite observations-driven modeling which is relevant to this work in the background research. Similar studies involving the effects of climate on total burned area should be noted by the authors, including Andela et al., 2017 and Zubkova et al., 2019.

The focus of this study is on machine-learning based prediction of wildfires and the relative importance of environmental controls of wildfires. Thus, the literature review was mainly focused on this aspect. However, we agreed reviewer's comments and added some references including the references mentioned by the reviewers.

(5)

Additionally, the methods section refers to aspects of the data which are not described until a later section.

As suggested, we have moved the data section (new section 2) before the model section (new section 3).

(6)

This organization is difficult for the reader to follow, and the description of the data used is insufficient, in part because the sources of the input data are not provided.

The sections have been rearranged as Data (section 2), Model (section 3), and Model validation and evaluation (section 4), Contributions of environmental factors to

predicted wildfire burned area (section 5), and Discussion and Conclusion (section 6). To better clarify the data sources, we have included them into the manuscript in section 2.

(7)

The data preprocessing methods are unclear as well – how is a discrete thematic variable like land cover type represented at 0.5-degree resolution?

The land cover type data is represented as 30 m x 30 m pixels with an assigned value to represent a given class of land cover type. We used the nearest neighbor resampling method to regrid the land cover type data onto the lower resolution of 0.5° x 0.5°. The nearest neighbor resampling method is illustrated in Figure R11. This method does not change any value from the original dataset but assigns the value to the new grid according to the value of the grid closest to the center of the new grid. This method was chosen because it is the fastest of the interpolation methods. For instance, compared to the nearest neighbor resampling, the majority resampling is relatively slow and time-consuming, because it is sensitivity to the size of the filter window and thus more experiments are required to determine the filter window. Additionally, since the it does not change the values of the cells, it is widely used for discrete data and it can keep the extreme values that are highly related to large fires (Baboo and Devi, 2010).

We applied the nearest neighbor resampling method to both continuous and discrete thematic variables to the 0.5° resolution. We have added the data preprocessing methods into the Data section (line 109-113).

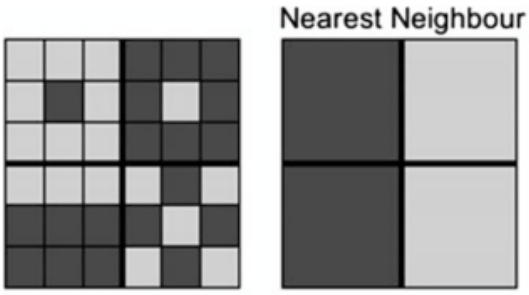

Fig. R11. Nearest Neighbor resampling technique. In this case, the nearest neighbor resampling is applied to grids with a resolution of 1x1 cell (left) to obtain grids with a resolution of 3x3 cell (right). (adopted from ESRI (2010)).

(8)

How are the translations between quantiles and area being made, given that the area of the grid cell varies with latitude?

The burned area of each grid cell was calculated by interpolating the fire data points into 0.5° grid cell based on their location. Although area of a grid decreases with latitude and higher latitude grids may contain fewer fire data points for interpolation, our interpolated burned area only depends on the magnitude but not the amount of the fire data points in a grid cell. Thus a higher latitude grid could have a large burned area despite its smaller grid area. For instance, we randomly sampled 10% of the grids from

two groups of grids for ten times: grids with latitude ranging from 26.75° to 28.25° (representing larger grids in lower latitude) and grids with latitude ranging from 35.25° to 36.75° (representing smaller grids in higher latitude). As Figure R12 shows, the grids in lower latitude ranging from 26.75° to 28.25° overall have smaller burned area, with the mean log of burned area of 1.28 ± 2.35 ha for the sampled grids, while the grids in higher latitude ranging from 35.25° to 36.75° generally have larger burned area, with the mean log of burned area of 2.18 ± 2.67 ha.

The above analysis supports the argument that a higher latitude grid could have a large burned area despite its smaller grid area. Given that our model can successfully capture burned area in a grid cell across various latitudes and burned area may not be dependent on grid area, our interpolated burned area distributions therefore need not be normalized to cater grid cells with different grid areas. When the quantile of the burned area distribution is predicted by the model, we just need to use the predicted quantile to extract the final predicted burned area from the distribution.

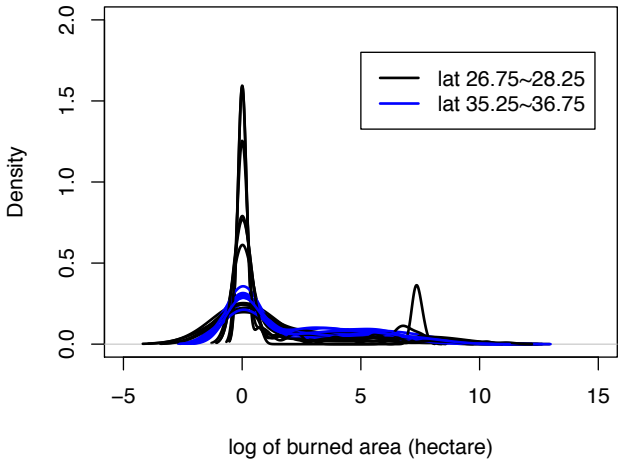

Fig. R12. Probability distribution of burned area for the randomly-selected grids in latitude range of 26.75° to 28.25° (black) and 35.25° to 36.75° (blue).

(9)
Also, the authors say the model predicts burned area at 50 km spatial resolution (with no indication of the map projection used), this is not the same as 0.5 degrees and this discrepancy needs to be resolved.
For this study, the point location of wildfire burned area was grouped into 0.5° grid cell based on their longitude and latitude. To avoid confusion, we have replaced the spatial resolution of '50km x 50 km' with '0.5° x 0.5°' throughout the manuscript.

(10) There are also questions about the fire data used to train the model – are prescribed fires included in the data (by definition, these are not wildfires in most cases)? Is there an estimate of the number of fires which are omitted?
The FPA-FOD fire data that we used excludes prescribed fires except for the prescribed fires that escaped their planned perimeters and became wildfires (Short, 2017). We have

clarified this in the manuscript (line 92-93).

Short (2014) compared FPA FOD data (1992-2011) with two national fire estimates from the US Department of Agriculture Forest Service (USFS) Wildfire Statistics and the National Interagency Coordination Center (NICC), which are available for 1992-1997 and 1998-2011, respectively. They showed that the annual number of fires estimated by FPA FOD is about 30% lower compared to that from the USFS estimation for the period of 1992-1997, as shown below (Fig. R13). The inconsistency of the fire number possibly may be caused by underestimation of small fires, as the fire burned area agrees well with USFS data. Our model will not be able to predict those small fires missing from the FDA-FOD as such information is not in the training dataset. The above discussions have been included in the text (line 93-98).

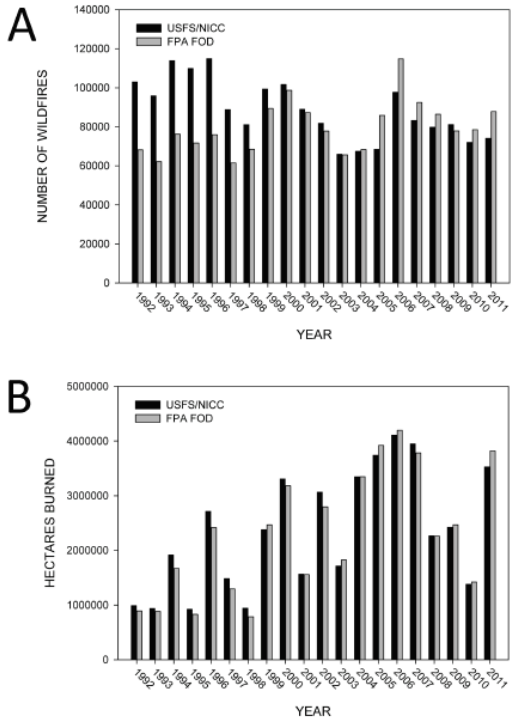

Fig. R13. Comparison of wildfire (a) numbers and (b) area burned area (hectares) in the US, 1992-2011, from published national estimates (USFS/NICC) and from FPA FOD. (adopted from Short et al. (2014); Fig. 4).

(11) Given the quantile-based approach, what happens if there is a fire or amount of burning which is greater than any in the training dataset (i.e. it would fall out of the range of the training data unless there was a training cell with 100% burned area)?

For a single grid, our four-step model can predict burned area greater than it had before based on its environmental conditions and by learning from other grids. However, random forest or quantile regression forest model cannot predict burned area larger than what it observed before from all the grids. For example, if the largest gridded burned area across the whole domain is 800 ha, the prediction for a single grid would never exceed 800 ha. Even though other methods such as MLR can predict burned area larger

than it observes before, there are some uncertainties in extrapolation (Amatulli et al., 2013; Mckenzie et al., 1996). We have included the above discussion in the manuscript (line 513-520).

(12)
Is the length of the training dataset long enough to capture all variability in fire activity as it relates to climatic conditions?
In 10-fold cross validation, the training dataset contains 16277 samples (It is derived from the total data length of 18085/10*9=~16277) for each fold for the winter-spring fire season. Assuming fire-climate relationships are unique for each individual grid, the large sample size is enough to capture all the variability in fire activity and its response to recent decadal climate. We have included this statement into the manuscript in line 429-432.

(13)
Why were remote sensing-derived datasets not considered?
We included satellite-derived monthly mean Leaf Area Index (LAI) obtained from MODIS instrument. In terms of fire data, since our focus is on wildfires and remote-sensing dataset does not separate prescribed fires from wildfires, we used FPA-FOD fire data instead of satellite-derived fire data such as GFED4 or FINN.

(14)
An important aspect of fire regimes which was not adequately considered in the manuscript is the role of human activity in the fire regime, especially in the United States where humans play an active role in the fire regime through suppression, ignitions, fuel load management, and landscape fragmentation in addition to being the source of ignition of approximately 85% of fires (according to the US Forest Service). These effects vary as function of not only population density, but sociopolitical norms which can vary from state to state. Recent papers such as the Andela et al. 2017 paper claim human activity is the major control on fire activity, and as such it cannot be ignored in a study region where the fire regime is likely human-driven. While the datasets describing human activity are certainly far from perfect, it is not possible to describe fire activity in a human-driven fire regime without considering human influences.
The focus of the paper is to quantify how environmental factors control wildfires in the study region under the present-day human management practices and human activities. Thus, we only included population density data of year 2010 to represent present-day human influence on wildfire activity. We acknowledge that population density is a rough estimate of effect of human activity on fires. We have included this statement into the manuscript in line 523-528.

(15)
Finally, there needs to be more effort in describing the expected impact of the work and the limitations of the method. For example, the abstract mentions that the work can be

used to assess fire management strategies but provides no details on how or why.
To clarify, the developed model aims to provide a broader impact on the community by accessing the quantitative contributions of the environmental controls of wildfires. An improved understanding of relative importance of the factors on wildfires would be useful for future fire prediction, fire management, as well as the linkage between wildfires and climate change. We removed the specific use of the model for fire management in the abstract and have restated the expected impact of the work and added the limitation of the method in the manuscript (line 510-537 and 558-567).

(16)
The quality of the input data is not discussed, which will propagate errors through the model, as well as the serial structure of the integrated model itself. At present, the manuscript is too focused on the machine learning exercise rather than on the scientific value of the work.
The discussion about the quality of the input data is added into the manuscript (line 520-523). Also, we have rewrote the manuscript to emphasize the scientific value of this work.

Specific Comments:
1. L75: Why were other months of the year excluded?
The total burned area of the two seasons accounts for 76% of the total annual burned area. As Fig. R14 shows, there are two peak seasons in South Central US: January to April and July to September. The dominance of wildfire occurrences in these months implies natural environmental conditions in these months are most conducive for wildfires. While wildfires do occur outside the fire seasons, their lower frequency implies that non-natural factors (e.g. human actions) can be relatively more important. As our study did not focus on human factors, we chose to exclude other months of the year. We have included the reason (line 74-79) and the Fig. R14 into the manuscript.

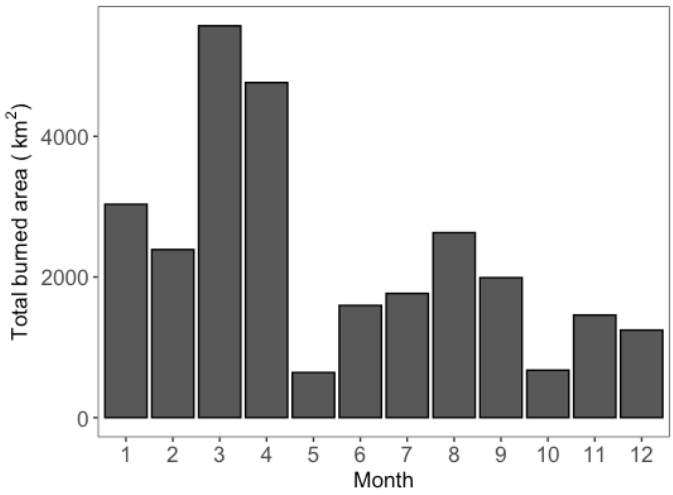

Fig. R14. Total burned area by month over South Central US. (This figure is now Fig. S1. In the revised manuscript)

2. L81: “Uneven data” is used throughout the paper but is not defined. Does this refer to unevenness spatially, temporally, or both?

It refers to both. The uneven distribution of burned area is defined as the situation where the number of grids with large burned areas is much smaller than the number of grids with small or zero burned areas. This situation exists for a single grid (temporal unevenness) and for all the grids within a given time period (spatially). The definition of unevenly-distributed burned area data has been included in the manuscript (line 57-59 and 182-183). An example of the uneven distribution of gridded burned area in winter-spring fire season is shown in Fig. R15. The Fig. R15 is included into the supplement to support the example of our case.

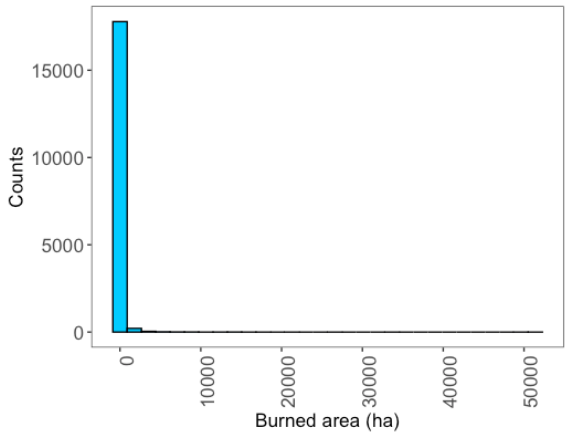

Fig. R15. Histogram of gridded burned area for the winter-spring fire season. (This figure is now Fig. S2a. In the revised manuscript)

3. L92-95: Given that the model compares the output to the quantile ranges, is it capable of estimating an amount of burning greater than has been observed in the training data?

See the response to general comment #11 above.

4. L155: Is there any concern about propagation of error through the model? What is the benefit of running three models in serial rather than one model alone or several models in an ensemble?

See the response to comment 6 for the reviewer 1, as shown below:

The reviewer is correct that biases from one step could be propagated to the subsequent steps, for example when the burned grids are predicted not to burn or when the unburned grids are predicted to burn. For the first case, when the burned grids are incorrectly predicted not to burn, the low bias is introduced because the burned grids would not proceed to step 3. For the second case, inclusion of unburned grids in step 3 may introduce a positive bias. We have included the discussions of the error propagation in section 6 (line 511-513).

To demonstrate our four-step model can achieve a higher accuracy and alleviate the issue of uneven-distributed dataset, we compare the prediction performance using

random forest alone with that of the four-step model developed in this study, as shown in the Table R3 below:

Table R3. Comparison of MAE and skewness between the RF model and the developed model (The information of this table is now included into the Table S2 in the revised manuscript)

Model	**RF alone**	**Model developed in this study**
MAE (winter-spring)	1.34	1.13
Skewness (winter-spring)	37.40 (burned area)	0.70 (quantiles)
MAE (summer)	0.70	0.57
Skewness (summer)	33.83 (burned area)	0.96 (quantiles)

Skewness is a measure of the asymmetry of the probability distribution of a random variable about its mean. The skewness of a random variable X is the third standardized moment $\widetilde{\mu_3}$, defined as:

$$\widetilde{\mu_3} = E\left[\left(\frac{X-\mu}{\sigma}\right)^3\right] = \frac{\mu_3}{\sigma^3} = \frac{E[(X-\mu)^3]}{(E[(X-\mu)^2])^{3/2}} = \frac{\kappa_3}{\kappa_2^{3/2}}$$

where μ is the mean, σ is the standard deviation, E is the expectation operator, μ_3 is the third central moment, and κ_t are the *t*-th cumulants. If skewness is less than -1 or greater than +1, the distribution is highly skewed. If skewness is between -1 and -0.5 or between +0.5 and +1, the distribution is moderately skewed. If skewness is between -0.5 and 0.5, the distribution is approximately symmetric. The positive value indicates that the tail is on the right side of the distribution while negative value indicates that the tail is on the left.

Our model has a lower MAE, by 15% and 19% for the winter-spring and summer fire season, respectively, compared to the single RF model. The distribution of the quantiles in the developed model is more uniform than the distribution of the burned area, as shown in Figure R6 below and the skewness. We have added a discussion of this issue in the text (line 355-365) and the Table R3 in the supplementary information. The information of skewness calculation has been included in the supplementary information. Note that we have replaced ‘quantile’ with ‘percentile’ in the manuscript to better clarify the idea of quantiles.

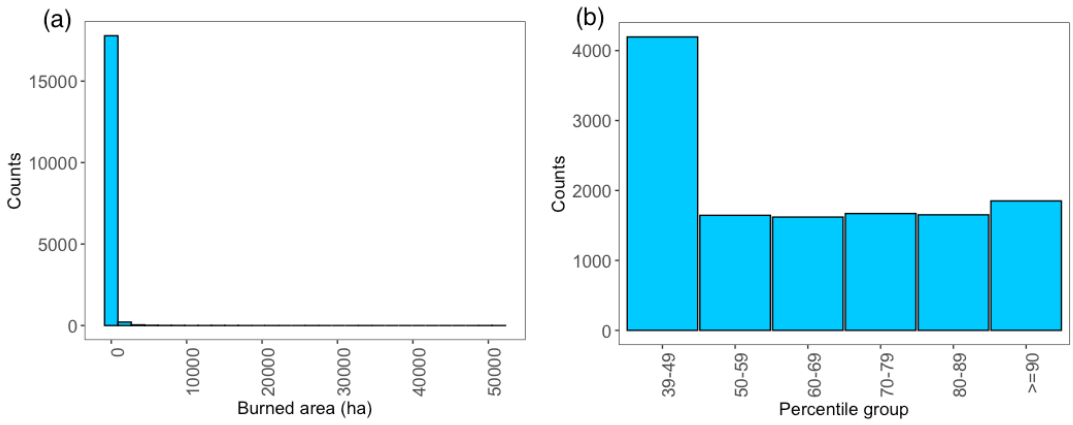

Fig. R6. (a) Histogram of burned area (b) Histogram of the percentile groups of burned area for the winter-spring fire season. (This figure is now Fig. S2. In the revised manuscript)

5. L164: Is there an estimate of the number of fires missed? Small fires constitute most of the fires by number, even though they add up to relatively little burned area (e.g. Malamud, Millington, and Perry 2005). It is noted that the dataset omits most small fires occurring on private land – these are not generally wildfires and such fires should be omitted anyways if the study is about wildfires.

See the response to general comment #(10) above.

6. L194-195: I don't think the climatic variables can be considered as fixed, especially since the assumption in later parts of the paper surround climate change scenarios which means their values do vary through time.

Climatic variables that are considered as fixed include only the mean and standard deviations of monthly meteorology over the past 22-years (1979-2000), because they do not vary by time over our study period (2002-2015) but characterize the spatial patterns of wildfire occurrence and intensity. The variables of climate anomaly are classified as climate variables (as opposed to fixed variables) since they are defined as the difference between monthly mean and the long-term average over 1979-2000 and their values vary by time. We have clarified this in the text (line 149-150 and line 435-440).

7. L209: Is any consideration given to preventing overfitting due the correlation between variables? For example, ecoregions and landcover types are likely to be related to one another.

Yes, we considered the collinearity of the variables when we designed the model. Thus, we chose logistic model and random forest model which work reasonably well under moderate collinearity (correlation coefficient < 0.7) (Dormann et al., 2013). We have added the concern of collinearity between variables into the text in line 213-215.

Although ecoregions and landcover types are likely to relate to one another, ecoregions represent large-scale areas comprised of similar biotic and abiotic phenomena while

land cover types are able to provide more detailed land information within one ecoregion. For example, in the temperate prairies (one ecoregion of our study domain), it has complex land types including pasture, woody wetlands, evergreen forest, and cultivated crops. Inclusion of these two variables allows us to capture fire responses to large-scale ecoregions and small-scale land types.

8. L232: Please clarify the phrase "horizontal scale of around 700 x 700 km2" – the use of horizontal scale implies a one-dimensional unit (length) which does not match the unit specified. Also, as a suggestion, 700 x 700 km2 seems ambiguous and could be more clearly represented as "700 km x 700 km" or "490,000 km2"
Good point. To avoid confusion, we have changed 'horizontal scale of around 700 x 700 km2' to 'spatial scale of around 700 km x 700 km'. The similar changes were also made for the Table S1.

9. L252: SUS is never defined
We have defined 'SUS' as 'southern US' for clarification.

10. L268-270: One could argue that the model is in fact "hardwired" (editorially, the term is jargon and should be replaced) to the geographical features of the study domain – geography deals with the human components of space and time as well as the physical components. The tendency of the human population to ignite or suppress fires as a result relationship to sociopolitical factors (like local regulations) will influence the fire regime in ways which will not be captured by climatic variables and will change from location to location.
We agreed with reviewer's point but the main focus of this paper is on how the environmental factors control wildfires in South Central US under the present-day human management practices and human activities. Therefore, the geographical features in the manuscript refer to coordinate variables such as longitude and latitude. To clarify this, we have replaced the term 'hardwired' and rewrote the corresponding paragraph in the manuscript (line 348-351).

11. L286: Why were 14 variables chosen? This seems like an arbitrary cutoff, especially given the large number of variables which went into the model.
We chose the top 14 variables because they represent the top quarter (25%) of the selected predictor variables. %IncMSE represents the change of mean square error with and without permuting variables. A larger %IncMSE value represents a higher variable importance. To see the sensitivity of the importance to the variable rank, we calculated the ratio of %IncMSE at variable ranked as X^{th} percentile (~top Y) to the %IncMSE at variable ranked as top (Y+1). Larger ratio means larger drop-off of the %IncMSE between topY and top(Y+1), which indicates notable decrease of variable importance at the cut-off point (top Y+1). We compared the ratio at several cutoff points: 25^{th} percentile, 50^{th} percentile, and 75^{th} percentile:

Table R6. The ratio of %IncMSE at variable ranked as X^{th} percentile (Y^{th}) to the %IncMSE at variable ranked as $(Y+1)^{th}$ for the three selected percentiles

	25% (Y=14)	50% (Y=29)	75% (Y=43)
Winter-spring fire season	1.21	0.88	1.00
Summer fire season	1.06	1.01	1.00

As the table shows, 25-percentile cut-off point has largest ratio, indicating a large drop of variable importance at the variable ranked 15^{th} and the top 14 variables have significantly larger importance. Thus, the top 25% variables (the top 14 variables) were chosen to be further discussed. The reasons of choosing the top 14 variables and associated discussions have been included in the manuscript (line 380-382). Table R6 has been added into the supplementary information as Table S4.

12. L306: The fuel-related variables are among the least important presented in Figure 5 – how can the conclusion be drawn that fuel abundance is what determines the amount of burned area?

Although fuel-related variables are among the least important in the top 14 variables, they are the fifth and sixth most important variables when excluding the fixed variables. Our conclusion was mainly based on the importance of time-varying variables. Therefore, burned area in the winter-spring fire season is mainly controlled by RH anomaly that directly affects fuel moisture. Besides that, the antecedent fuel abundance and pre-fire-season drought conditions together determines the amount of dry fuel in the winter-spring fire season. To clarify this, we have rewritten the corresponding paragraph in line 407-410.

13. Table 1: The resolution of the data is presented, but it's not clear how the data are being re-gridded to the working resolution - if the fire analysis is being done at 0.5 degree and the climate data is at 32 km resolution then there are < 4 cells per burned area data point and the way which those 4 cells are represented has significant consequences.

See the response to general comment #(7) above.

References:

Amatulli, G., Camia, A. and San-Miguel-Ayanz, J.: Estimating future burned areas under changing climate in the EU-Mediterranean countries, Science of The Total Environment, 450–451, 209–222, doi:10.1016/j.scitotenv.2013.02.014, 2013.

Baboo, S. and Devi, R.: An Analysis of Different Resampling Methods in Coimbatore, District, Global Journal of Computer Science and Technology, 10(15), 61–66, 2010.

Dormann, C. F., Elith, J., Bacher, S., Buchmann, C., Carl, G., Carré, G., Marquéz, J. R. G., Gruber, B., Lafourcade, B., Leitão, P. J., Münkemüller, T., McClean, C., Osborne,

P. E., Reineking, B., Schröder, B., Skidmore, A. K., Zurell, D. and Lautenbach, S.: Collinearity: a review of methods to deal with it and a simulation study evaluating their performance, Ecography, 36(1), 27–46, doi:10.1111/j.1600-0587.2012.07348.x, 2013.

ESRI: Manual ArcGIS [software GIS] Version 10, Environmental System Research Institute, Inc., 2010.

Mckenzie, D., Peterson, D. L. and Alvarado, E.: Extrapolation Problems in Modeling Fire Effects at Large Spatial Scales: a Review, Int. J. Wildland Fire, 6(4), 165–176, doi:10.1071/wf9960165, 1996.

Short, K. C.: A spatial database of wildfires in the United States, 1992-2011, Earth System Science Data, 6, 1–27, doi:10.5194/essd-6-1-2014, 2014.

Short, K. C.: Spatial wildfire occurrence data for the United States, 1992-2015, Forest Service Research Data Archive (4th Edition), doi:10.2737/RDS-2013-0009.4, 2017.

Quantifying the effects of environmental factors on wildfire burned area in South Central US using integrated machine learning techniques

Sing-Chun Wang[1], Yuxuan Wang[1]

[1]Department of Earth and Atmospheric Sciences, University of Houston, Houston, Texas 77024, USA

Correspondence to: Yuxuan Wang (ywang246@central.uh.edu)

Abstract. Occurrences of devastating wildfires have been increasing in the United States for the past decades. While some environmental controls, including weather, climate, and fuels, are known to play important roles in controlling wildfires, the interrelationships between these factors and wildfires are highly complex and may not be well represented by traditional parametric regressions. Here we integrate multiple machine learning algorithms to develop a prediction model of 0.5°x0.5°-gridded monthly wildfire burned area over the South Central United States during 2002-2015 and then use this model to identify the relative importance of the environmental drivers on the burned area for both the winter-spring and summer fire seasons of that region. The developed model alleviates the issue of unevenly-distributed burned area data, predicts burned grids with Area Under the Curve (AUC) of 0.82 and 0.83 for the two seasons, and achieves temporal correlations larger than 0.5 for more than 70% of the grids and spatial correlations larger than 0.5 ($p<0.01$) for more than 60% of the months. For the total burned area over the study domain, the model can explain 50% and 79% of the observed interannual variability for the winter-spring and summer fire season, respectively. Variable importance measures indicate that relative humidity (RH) anomalies and preceding months' drought severity are the two most important predictor variables controlling the spatial and temporal variation of gridded burned area for both fire seasons. The model represents the effect of climate variability by climate-anomaly variables and these variables are found to contribute the most to the magnitude of total burned area across the whole domain for both fire seasons. In addition, antecedent fuel amount and conditions are found to outweigh the weather effects for the magnitude of total burned area in the winter-spring fire season, while fire weather is more important for the summer fire season likely due to relatively-sufficient vegetation in this season.

1. Introduction

Wildfire is an important process maintaining the balance of terrestrial ecosystems. Wildfire occurrence is controlled by a complex interaction among fuel, weather, and climate (Bowman et al., 2009; Pausas and Keeley, 2009). In recent decades, many regions of the world have experienced an increase in frequency and intensity of wildfires, which may be possibly connected to changes in regional climate (Barbero et al., 2015; Westerling et al., 2006; Westerling, 2016). More intense and more frequent wildfire activities not only heighten ecosystem vulnerability but also cause poor air quality (Jaffe et al., 2008;

Pellegrini et al., 2017; Wang et al., 2018; Yue et al., 2015). Thus, it is imperative to understand how wildfires would respond to changes in environmental factors in a warming climate.

Previous studies revealed the importance of several environmental factors on wildfires. Fuel availability and composition across regions can affect fire developments such as fire likelihood and spread efficiency (Nunes et al., 2005; Parks et al., 2012). Weather influences fuel moisture by changing precipitation and humidity and controls fire spread through winds. Long-term climate change can alter both fuel and weather conditions, for example by adjusting vegetation distributions and the frequency of fire-favorable atmospheric conditions (Heyerdahl et al., 2008; Keyser and Westerling, 2017; Morgan et al., 2008; Zubkova et al., 2019), therefore changing fire regimes. Past studies also highlighted that the complex interplay between fuel, weather, climate, and wildfires can change by spatial scale, fire size, region, and season. For instance, the relationships between fire activity and the environmental controls can exhibit complex nonlinearities across the spatial scale gradient (Peters et al., 2004). Fuel and topography mainly regulate fires at a local scale, while weather and climate control fires at a broad spatial scale (Parks et al., 2012). In terms of fire size, it was found that the major controlling factors could shift from fuel and topography to weather as fire size increases in boreal forests (Liu et al., 2013; Fang et al., 2015). In the western Mediterranean Basin where land heterogeneity is large, influences of fuel can outweigh influences of climate and weather on large fires (Fernandes et al., 2016). Therefore, it is challenging to examine the relative importance of the environmental drivers on wildfires due to the complex interrelationships among them.

One common method to explain the relationships between fire regimes (e.g. fire sizes or fire occurrences) and environmental factors is regression. This method is also used to evaluate the relative importance of different environmental controls (Littell et al., 2009; Slocum et al., 2010; Parisien et al., 2011; Yue et al., 2013; Liu & Wimberly, 2015; Fernandes et al., 2016). Among a wide range of regression techniques used, non-parametric machine learning algorithms have emerged as an important tool to predict wildfires because they rely on fewer pre-assumptions about the data. Bedia et al. (2014) used non-parametric multivariate adaptive regression splines (MARS) to model the monthly burned area for the phytoclimatic zones in Spain of sizes ranging from 25 km x 25 km to 100 km x 100 km. Amatulli et al. (2013) used two machine learning approaches, Random Forest (RF) and MARS, to estimate monthly burned area in five countries in Europe with a spatial resolution ranging from 300 km x 300 km to 1000 km x 1000 km. In these studies, the machine learning methods were used to estimate total burned area aggregated over a large-scale domain, e.g. on an ecoregion or a country scale (Table S1). However, fewer studies have explored the utility of machine-learning methods in resolving the within-domain and grid-level relationships between fires and the environmental drivers. A particular challenge in predicting burned area of fires at the grid level across a broad region relates to the uneven distribution of burned area both spatially and temporally, where the number of grids of large burned area is much smaller than the number of those with small or zero burned areas. For example, Steel et al. (2015) showed that for fires in California, small fires (< 25 ha each) contributed to 87% of the total number of grids burned but only 17% of the total burned area, whereas large fires (> 150 ha each) accounted for only 3% of the total number of burned grids but made up 64% of the total burned area. Thus, at the grid level the majority class is non-burn wildlands or small fires, while the

minority class is large fires. As most data-driven regression algorithms, parametric or non-parametric, would favor the majority class, large fires will be underpredicted for grid-level predictions.

In this study, we develop a model integrating multiple machine learning techniques to predict wildfire burned area at the grid level over South Central United States (US), which encompasses four states: Texas, Oklahoma, Louisiana, and Arkansas. This region has experienced periodically large wildfires in recent years, such as the 2011 Texas fires (Long et al., 2013; Nielsen-Gammon, 2012). It is also projected to have the highest risk of wildfires in 2031-2050 across the continental US (An et al., 2015; Fann et al., 2018). The integrated machine learning model aims at mitigating the problem of uneven burned area and improving the accuracy of predicting wildfire burned area at a grid-scale of 0.5° x 0.5°. Using the prediction model developed here, the goal of this paper is to estimate the relative importance of different environmental factors on wildfire burned area in the study region which would be useful for future fire prediction as well as the linkage between wildfires and climate change. We chose the vegetation-rich thus fire-prone part of the South Central US, as shown by the red box in Figure 1. The study period is from 2002 to 2015. For each year, we predict gridded wildfire burned area at the monthly scale for the typical bimodal wildfire seasons over the region (Figure S1): the winter-spring fire season from January to April and summer fire season from July to September (Zhang et al., 2014). These two seasons contribute 76% of the annual total burned area, indicating that natural environmental conditions in these months are most conducive for wildfires. While wildfires do occur outside the fire seasons, their lower frequency implies that non-natural factors (e.g. human actions) can be relatively more important. As our study did not focus on human factors, we chose to exclude other months of the year.

The rest of the paper is organized as follows: Section 2 introduces data incorporated into the model. Section 3 describes the developed model and validation method. Section 4 presents the results of model validation and evaluation. In section 5, we analyze the relative importance of individual variables and the environmental controls at different spatial scales. Discussion and conclusion are given in section 6.

2. Data

2.1 Wildfire burned area

The model predicts wildfire burned area at a grid-scale of 0.5°×0.5° over the study region. Wildfire burned area is chosen as the target variable because it is a widely-used parameter for quantitative assessment of fire danger and fire impact (Amatulli et al., 2013; Balshi et al., 2009; Yue et al., 2013). Wildfire information over the study period (2002-2015) was obtained from the Fire Program Analysis Fire-Occurrence Database (FPA-FOD). The FPA-FOD collects daily wildfire reports from federal, state, tribal, and local governments. The dataset includes wildfire burned area, fire location in longitude and latitude, and fire discovery date from 1992 to 2015 (Short, 2017). The FPA-FOD fire data excludes prescribed fires except for the prescribed fires that escape their planned perimeters and become wildfires. A known caveat of this database is that it does not include some small fires that occur on private lands. Short (2014) reported that for the period of 1992-1997 the national

total number of wildfires from the FPA-FOD is about 30% lower compared to that from the US Department of Agriculture Forest Service (USFS) Wildfire Statistics, although the national total burned area is consistent between the two datasets. Thus, our model will not be able to predict those small fires missing from the FDA-FOD as such information is not in the training dataset.

The FPA-FOD wildfire data is point data at a daily time step. As the prediction model deals with monthly total burned area at a spatial resolution of 0.5°×0.5°, we aggregated the daily point burned area into 0.5°×0.5° grid cells based on fire longitude and latitude and summed the burned area in each grid by month. The resulting dataset of monthly burned area has nearly 70% of the grids with burned area less than 10 ha or non-burned. To reduce skewness and improve data symmetry, we applied the log transformation function $ln(x+1)$, where x is the gridded monthly total burned area. The log-transformed burned area was the target variable of the model.

2.2 Predictor variables

Based on previously published studies, we collected a number of predictor variables that are thought to influence wildfire burned area (Fang et al., 2015; Keyser and Westerling, 2017; Liu and Wimberly, 2015; Riley et al., 2013; Yue et al., 2013) and grouped them into four categories of environmental controls (Table 1): weather, climate, fuel, and fixed-geospatial variables. These predictor variables are listed in Table 1 and described below. All the variables, including continuous and discrete thematic variables, were resampled to spatial resolution of 0.5°× 0.5° by the nearest neighbor resampling method (Baboo and Devi, 2010). The nearest neighbor resampling method assigns a value to the new grid according to the value of the original grid closest to the center of the new grid. The resampling method has the advantages of being efficient and not changing any value from the original dataset.

2.2.1 Weather variables

The meteorological data were obtained from the North American Regional Reanalysis (NARR) with a spatial resolution of 32 km x 32 km. The weather variables include the monthly total accumulated precipitation and the monthly means of the following variables: daily precipitation, daily average and maximum temperature, zonal (U) and meridional (V) components of wind at 10 m, and daily average and minimum relative humidity (RH). In order to select extreme conditions that are likely to induce wildfires on a sub-monthly time scale, we also included the number of consecutive days without rainfall within a month, which is based on daily precipitation from the NARR data. Another extreme weather pattern conducive for wildfires is drought. Drought depicts the extreme condition of water deficit in the coupled land-atmosphere system that can be driven not only by lack of precipitation but also by excessive evaporation. We used the Standard Precipitation and Evaporation Index (SPEI) to represent drought intensity (Vicente-Serrano et al., 2009). The SPEI incorporates both precipitation and potential evapotranspiration to estimate climatic water balance at different time scale (1 to 48 months). In this study, we used the 1-month SPEI from the global SPEI database (http://spei.csic.es/database.html) with a spatial resolution

of 0.5°× 0.5°. Positive values of SPEI represent wetter than normal conditions and negative values indicate situations that are drier than normal conditions.

Weather conditions in the preceding months are also known to influence fire development. For example, an increase of precipitation in the preceding months can promote biomass growth and provide fuels for a widespread of larger wildfires in a later month (Fréjaville and Curt, 2017; Littell et al., 2009). To consider such lagged effects, for a given month *t*, we calculated the averages of the aforementioned weather variables from the months *t-1* to *t-12*. We then included those lagged variables that have correlation coefficients (r) larger than 0.5 with wildfire burned area of month *t* but are not strongly correlated with the same variables of month *t* ($r < 0.5$). For the winter-spring fire season, the antecedent variables that pass this criterion are the monthly mean of daily precipitation of months *t-1* and the average SPEI of the months *t-1*, *t-1* to *t-2*, *t-1* to *t-3*, *t-1* to *t-4*, *t-1* to *t-5*, and *t-1* to *t-6*. For the summer fire season, the selected antecedent variables are the average of monthly mean temperature for months *t-1* and *t-1* to *t-2*, monthly mean of daily precipitation for months *t-1, t-1* to *t-2* and *t-1* to *t-3*, and mean SPEI of months *t-1*, *t-1* to *t-2*, and *t-1* to *t-3*.

2.2.2 Climate variables

Inputs of climate variables to the model include both climate anomalies and 22-year (1979-2000) means and standard deviations of selected meteorological variables. Here climate anomalies refer to the departure of monthly mean meteorological variables from their long-term averages over 1979-2000, thereby representing the effects of climate change on meteorological conditions. The climate anomalies were calculated for the monthly total precipitation and monthly means of daily average precipitation, daily average and maximum temperature, average and minimum RH. The long-term average and standard deviation of meteorological variables characterize the spatial and temporal patterns of the mean climate conditions, which can determine the typical vegetation of the study region and hence influence fire occurrence and size (Keyser and Westerling, 2017). We used the 22-year means and standard deviations of monthly total accumulated precipitation and monthly means of daily average and maximum temperature, and daily average precipitation. As climatological means and standard deviations do not vary with time, they are grouped with the geospatial variables later in the study as the category of fixed variables.

2.2.3 Fuel variables

Fuel variables were selected to estimate the fuel effect on burned area and these variables include monthly mean of Leaf Area Index (LAI), sum of neighboring LAI, and soil moisture. The LAI is the ratio of the total one-sided area of green leaf area per unit ground surface area, which has been widely used to describe the structural property of a plant canopy. Additionally, LAI is correlated with important metrics of canopy fuel loads, such as canopy bulk density (Keane et al., 2005; Steele-Feldman et al., 2006). The monthly mean LAI at a spatial resolution of 500 m was obtained from MODerate resolution Imaging Spectroradiometer (MODIS) instruments. Besides local LAI values, to capture the effects of spatial autocorrelations,

we consider each grid cell as the center of a 3-by-3 grid matrix and compute the summation of the LAI from the center grid's eight neighboring grids. This summation is referred to as the 'sum of neighboring LAI' and included as a predictor variable. The lagged effects of fuel buildup in the preceding months are expected to influence wildfire occurrence and size. Using the same criteria to select antecedent weather variables (section 2.2.1), the averages of LAI and sum of neighboring LAI for the months *t-1* to *t-6* were selected as antecedent fuel variables for the winter-spring fire season, but no such variables were included for the summer fire season because none passed the selection criteria.

Fuel moisture is a critical property for evaluating fire danger. As fuel moisture data is limited, soil moisture is often used as an indicator for fuel moisture because of the strong correlation between the two (Krueger et al., 2016). Here, we used the monthly surface soil moisture (0-10 cm) from the Noah land-surface model for Phase 2 of the North American Land Data Assimilation System (NLDAS-2) with a spatial resolution of 0.125°× 0.125° to represent the influence of fuel moisture.

2.2.4 Geospatial variables and population

Lastly, population and two geospatial variables were used as predictors, including land cover types and ecoregion types. Land cover types and ecoregion types were chosen to capture the effects of land use and ecosystem similarity on wildfire burned area. The land cover data at the spatial resolution of 30 m was obtained from the 2011 Landsat-derived land cover map from the National Land Cover Database (NLCD) (https://www.mrlc.gov). The ecoregion data was obtained from EPA (https://www.epa.gov/eco-research/ecoregions). The ecoregions denote areas of similarity in the mosaic of biotic, abiotic, terrestrial, and aquatic ecosystem components. Population density data in the year 2010 from the U.S. Census Bureau (https://www.census.gov/geo/maps-data/data/tiger.html) was used to estimate the influence of present-day human management practices and human activities on wildfires.

3. Model

3.1 Model description

One major challenge in wildfire prediction is the highly uneven distribution of burned area where the number of grids with large burned areas is typically much smaller than the number of grids with small or zero burned areas (Figure S2a). For the study region (red box in Figure 1), grids without any fire occurrence in combination with those of only small fires (< 25 ha) take up 79% of the total number of the grids but correspond to only 1% of the total burned area. By contrast, grids with large burned area (>150 ha) account for 84% of the total burned area but only 6% of the total number of grids. For such unevenly-distributed data, standard machine learning methods usually favor the majority class (i.e. non-burned or small fires), leading to low prediction accuracy of the minority class (i.e. large fires) (Krawczyk, 2016). To alleviate the low bias toward large fires, we developed a model consisting of multiple steps that address the uneven data issue.

Figure 2 demonstrates the structures and processes of our model, which has four steps and uses three machine learning algorithms. First, for each data grid, given the predictor variables, we use the quantile regression forest (QRF) to predict a distribution of burned area at the targeted percentiles which are chosen at 45, 55, 65, 85, 95, and 99 in this step. The percentiles here refer to the relative position of the predicted burned area in the cumulative distribution of all the burned area data and they were chosen to include the whole conditional distribution. Second, for all the grids, we predict if a grid burns or not by using the logistic regression model and the same set of predictor variables as in the first step. Third, for the grids that are predicted to burn, instead of predicting burned area directly, we use a random forest (RF) model to predict the percentile of burned area relative to the training set. After all the predicted-burn grids obtain their predicted percentiles of burned area by the RF, the test dataset is divided into six sub-groups according to their predicted percentiles: {(39,49), (50,59), (60,69), (70,79), (80, 89), (>=90)}. The percentile groups were chosen to align with the six percentiles in the first step. The first three percentiles correspond to the median of the first three percentile groups. For example, the first percentile group (39, 49) has a median percentile of 45, the first percentile of predicted wildfire burned area from the first step. The last three percentiles (85, 95, and 99) from the first step correspond to the last three percentile groups of (70, 79), (80, 89), and (>=90), respectively, although they lie outside the upper bounds of corresponding subgroups. This is based on the assumption that grids with larger predicted burned area (predicted percentile > 70) in the testing set will have more right-shifted burned area distributions than the distributions of the whole training set, as shown in Figure S3. In step 4, for the grids in a given subgroups, they are assigned to the burned area value at the corresponding percentiles as determined by the predicted distribution generated from the first step. Specifics of the machine learning algorithms and technical details of the prediction model are described in the subsections below.

Our approach alleviates the unevenness data issue for two reasons. First, the majority of zero-burn grids are separated by the second step. Second, for the grids predicted to burn, we predict the relative position (i.e. percentiles) of the burned area based on the training set. As Figure S2 and Table S2 show, the distribution of percentiles is less skewed compared to the burned area distribution. Thus, the unevenness of the burned area is less severe when predicting the percentiles than predicting the burned area directly. Given the possible collinearity between the predictor variables, we chose the logistic model and RF model which are shown to work reasonably well under moderate collinearity (correlation coefficient < 0.7) (Dormann et al., 2013). We verified that the correlation between any pairs of the predictor variables is less than 0.7.

3.1.1 Random forest regression

Random forest (RF) is an ensemble-learning algorithm built on decision trees. Each tree is built using the best split for each node among a subset of predictors randomly selected at the node (Liaw and Wiener, 2002). The best split criterion is based on selecting the variables at the nodes with lowest Gini Index (GI), which is defined as GI $(t_x(x_i))$ = 1- $\sum_{j=1}^{m} f(t_x(x_i),j)^2$, where $f(t_x(x_i),j)$ is the proportion of samples with the value *xi* belonging to leave *j* as node *t*. Two parameters can be adjusted to optimize the RF model, including the number of trees grown (n_{tree}) and the number of predictors sampled for splitting at each node (m_{try}). The RF regression model first draws n_{tree} bootstrap samples from the original dataset.

For each sample, at each node of a tree, m_{try} predictors are randomly chosen from all the predictors and then the best split from among the predictors is determined at each node according to GI. In this study, we had n_{tree} of 1200 and m_{try} of 8 for the winter-spring fire season and n_{tree} of 1500 and m_{try} of 7 for the summer fire season to obtain the best prediction accuracy. The predicted value of an observation is the average of the observed values belonging to the leaves of n_{tree} trees. Here, we used RF model to predict percentiles of burned area for the grids that were predicted to burn.

The benefit of applying the RF model is that it can provide the variable importance that measures the strength of individual predictors. The variable importance is measured by the increase in the mean square error (%IncMSE) and the increase in node purities (IncNodePurity). The %IncMSE is calculated by comparing the mean square error with and without permuting variables for each tree, and the variables with greater values of %IncMSE are more important. As for the IncNodePurity, the changes of residual sum of square (RSS) before and after the split are first derived at each split, and the final IncNodePurity of a variable is obtained by summing over the RSS of all the splits that include the variable over all trees. Thus, a larger IncNodePurity represents a higher variable importance.

3.1.2 Quantile regression forests

Quantile regression forests (QRF) are an extension of the RF (Meinshausen, 2006). QRF develops trees in the same way as RF, but instead of calculating the average of the values from leaves of the trees to obtain a single predicted value, the QRF estimates the conditional distribution of a target variable. The conditional distribution is calculated by averaging the conditional distributions from all the trees and the predicted quantiles or percentiles are derived from the final empirical distribution function. Here we chose to predict percentiles at 45, 55, 65, 75, 85, 95, and 99 as described above. These percentiles were selected because they can represent the full spectrum of fire sizes ranging from small to extremely large ones. The percentiles less than 45 are typically zero-burn, so the percentile of 45 is the lowest percentile that can possibly record both zero-burn and very small burned area for each grid.

3.1.3 Logistic regression model

Logistic regression is used to estimate the probability of wildfire occurrences in a grid cell by the statistical relationships between wildfire occurrences and the predictor variables. Logistic regression is defined as $P_i = \frac{1}{1+e^{-\eta i}}$ and $\eta_i = \beta_0 + \beta_1 X_{i1} + \beta_2 X_{i2} + \cdots + \beta_\rho X_{i\rho}$, where Pi represents the probability of an occurrence of wildfire in a grid cell i, η_i is the linear combination of the predictor variables weighted by their regression coefficients (β), x_{ij} is the value of the predictor variable j of the grid i, and β_0 is the constant. The logit function can be expressed as $\log\left(\frac{P}{1-P}\right) = x_i^T \beta$, where x_i^T is the vector of the predictor variables and β is the vector of the parameters. Values of P larger than 0.4 are considered to be an occurrence of wildfires and those equal to or less than 0.4 are interpreted as nonoccurrence of wildfires. If a grid is classified not to burn,

the predicted burned area is zero and that grid will not be processed further. On the other hand, if a grid is classified to burn, it would be analyzed by the RF model to predict the burned area percentiles.

3.2 Validation method

We applied a 10-fold cross-validation (CV) technique to evaluate the model performance and to avoid overfitting. The entire dataset (2002-2015) was randomly divided into 10 equal-sized splits. For each round of CV, the model was trained with nine splits of the data and the trained model was then used to predict burned area at the remaining split.

Classification of burned or unburned grids was evaluated by the accuracy, precision, recall, and F1-score. Precision and Recall are defined in Equation (1) and (2):

$$Precision = \frac{True\ positive}{True\ positive + False\ positive}, \quad (1)$$

$$Recall = \frac{True\ positive}{True\ positive + False\ negaitve}, \quad (2)$$

where true positive is the number of burned grids correctly predicted, false positive is the number of grids which are unburned but are predicted as burned, and false negative is the number of grids which are burned but are predicted not to burn. The F1 score measures a model's accuracy that combines precision and recall:

$$F1 = \frac{2}{recall^{-1} + precision^{-1}}, \quad (3)$$

F1 score has a maximum value of 1 and minimum value of 0, and the higher F1 indicates a higher balance between Precision and Recall. In addition to the aforementioned evaluation criteria, we used receiver operating characteristic (ROC) curve, and the area under the curve (AUC) statistics to evaluate the classifier (Metz, 1978). The ROC curve shows how well the model can distinguish between the true positive rate (TPR) and the false positive rate (FPR), where TPR and FPR are expressed by Equation (4) and (5):

$$True\ positive\ rate = \frac{True\ positive}{True\ positive + False\ negative}, \quad (4)$$

$$False\ positive\ rate = \frac{False\ positive}{False\ positive + True\ negative}, \quad (5)$$

The AUC is the area under the ROC curve and it ranges from 0 to 1. The greater the AUC, the better discrimination between true positive and true negative.

Burned area predictions were evaluated using statistical indicators such as the coefficient of determination (R^2), mean absolute error (MAE), and root mean squared error (RMSE) between the predicted and observed wildfire burned areas. The evaluation was done for the winter-spring fire season and summer fire season separately. The prediction performance was also quantified in terms of the model ability in reproducing temporal variation of burned area for each grid and spatial patterns of burned area across all the grids of the study domain. Details on the calculation of the spatial and temporal correlations are described in the Supporting Information.

4. Model validation and evaluation

Here we present the validation results at two spatial scales: the grid-scale of 0.5°× 0.5° and the large-domain scale of 700 km x 700 km corresponding to the size of the study domain (red box in Figure 1). The grid-scale prediction of all possible outcomes (i.e., unburned, small burned, and large burned area) is a unique strength of our model. To the best of our knowledge, none of previously published studies included unburned and small burned grids into the prediction of wildfire burned area at a grid scale as fine as 0.5°× 0.5°. At the large-domain scale, we will compare our model performance with prior studies which predicted total burned area of an ecoregion or a country.

Table 2 lists a variety of statistics representing the model performance at the grid-scale for the winter-spring fire season and summer fire season. The prediction performance of the classifier (i.e. the second step in the model) was evaluated by the ROC curves (Figure S4), the area under the ROC curve (AUC), accuracy, recall, precision, and F1-score. The ROC curves of both fire seasons steer toward the upper left corner, indicating a good performance of the model with a high detection rate of fires and a low false alarm. The AUCs for the two fire seasons are 0.82 and 0.83. The accuracy and F-1 score are 0.74 and 0.79, respectively for the winter-spring fire season and 0.74 and 0.77 for the summer fire season. These results indicate the model is capable of classifying burned grids and unburned grids with a good balance of recall and precision.

In terms of burned area prediction at the grid scale, the R^2 reached 0.42 and 0.40 for the winter-spring and summer fire season respectively. MAE and RMSE are 1.13 and 8.37 respectively for the winter-spring fire season, and 0.57 and 4.26 for the summer fire season. Before comparing these prediction statistics with previously published studies that predicted gridded burned area, it is important to note that the prediction accuracy will depend on the temporal scale (e.g. monthly or annual) and grid resolution at which the prediction is made. The larger spatiotemporal scales are expected to have a better prediction performance. Regarding the type of grids to be predicted, the most challenging case is the prediction including all possible outcomes of a given grid (i.e., unburned, with small burned areas, and with large burned areas). As fewer prior studies of the similar nature as ours predicted all possible outcomes (i.e. not only large burned areas but also unburned and small burned cases) at the grid-level and none of these studies targeted the South Central US, we chose to compare our model performance with previously published models that predicted gridded burned area in terms of the approaches, the temporal and spatial resolution, and the percent of variance explained by the model, regardless of their study regions, periods, methods, and predictors. Chen et al. (2016) used ocean climate indices to estimate annual burned area at the grid resolution of 1° x 1° but their prediction was only for those grids with non-zero annual burned area. They achieved a prediction R^2 of less than 0.3 (correlation coefficient r around 0.55) over the southern US (SUS). Using boosted regression trees, Liu and Wimberly (2015) obtained a higher R^2 of 0.76 between climate variables and burned area over the western US, but their investigation was limited to only extremely large fires (> 405 ha) and was at a 1° x 1° resolution and annual timestep. Compared to those studies, our model targeted a more challenging prediction (i.e. prediction at a finer spatial and temporal scale and for all the grids), yet achieved a comparable if not better performance at the grid scale.

Considering there were very few studies that predicted burned area by grids and at the same time considered unburned grids or grids with small fires, we extended the comparison to past studies predicting burned area of regions with the similar spatial scales of 0.5° x 0.5°. Urbieta et al. (2015) used Multiple Linear Regression (MLR) to predict annual burned area of provinces and national forests in the southern countries of the European Union (EUMED) and Pacific Western US (PWUSA), with the mean domain size of 108 km x 108 km. Their reported median R^2 is 0.28 for EUMED and 0.22 for PWUSA, smaller than our value (0.4). Using the MLR method, Carvalho et al. (2008) predicted monthly burned area of Portuguese districts of sizes ranging from ~ 25 km x 25 km to 100 km x 100 km and their R^2 is between 0.43 to 0.80. The better model performance was only for some districts with evenly-distributed burned area, whereas the districts with highly right-skewed burned area distributions (Evora and Portalegre) had prediction R^2 of 0.43~0.45. Bedia et al. (2014) predicted monthly burned area of phytoclimatic zones in Spain (~25 km x 25 km to 100 km x 100 km) by using multivariate adaptive regression splines (MARS) and obtained R^2 ranging from 0.01 to 0.37. In comparison with these results, the R^2 of 0.42 and 0.40 that we achieved for the two fire seasons at a grid resolution of 0.5° x 0.5° is a significant improvement for situations with unevenly-distributed burned area. In addition, by predicting all possible outcomes for all the grids within a large domain, our model framework would be more flexible and practical to be applied to other domain.

The aforementioned statistics demonstrate the general capability of our four-step model in predicting gridded burned area over the study period. We selected three specific years to further illustrate the model performance: 2011 with the largest domain-mean gridded burned area, 2008 and 2014 with the domain-mean gridded burned area close to the 14-year-mean for the winter-spring and summer fire season respectively. Figure 3 shows the selected CV-predicted and observed monthly burned area of these years for each fire season. The R^2 is 0.42, 0.51, and 0.66 for 2011 (combing both seasons), 2014 (the winter-spring season), and 2008 (the summer fire season), respectively, after excluding misclassified grids. MAE of 2011, 2014, and 2008 are 5.25, 0.77, 0.43 and RMSE are 21.06, 5.87, and 1.75. The detailed statistics of the model performance for each year are shown in Table S3. The results show that the model has a better performance in predicting gridded burned area for normal years of 2008 and 2014 than for the exceptionally large wildfire year of 2011. For 2011, large burned area can be well modeled but small burned area (log of burned area < 2) is overpredicted. This can be explained by the fact that the extremely hot and dry weather during 2011 caused fire-favorable conditions across the study domain. Due to the lack of reliable and detailed information about ignition and suppression, it is difficult for the model to discriminate between small and large fires given widespread extreme drought conditions across the whole domain during 2011 (Long et al., 2013; Nielsen-Gammon, 2012).

The model performance was further evaluated in terms of its ability in reproducing the spatiotemporal patterns of monthly mean burned area for the two fire seasons (Figure 4). The correlation coefficient between the 14-year mean observed and predicted burned area is 0.82 and 0.80 for the winter-spring and summer fire season, respectively. For the whole study period, more than 60% of the months have a spatial correlation larger than 0.5 for both fire seasons between the observed and predicted monthly burned area. It is noteworthy that such performance is achieved without introducing any coordinate variables like longitude or latitude as predictors. This indicates the chosen predictors contain sufficient information to capture the spatial heterogeneity of the environmental factors and thus the framework of the model could be easily adopted for other regions,

making it possible to be incorporated into climate models in future applications. Temporally, more than 70% of the grids have a correlation higher than 0.5 between the observed and predicted time series of burned area (combined the two fire seasons) (Figure S5). These results demonstrate the model has a certain ability in predicting both spatial and temporal variation of the burned area at the grid-scale across the study domain.

Even though bias may be introduced in the multi-steps model, the developed four-step model can achieve higher accuracy and alleviate the issue of uneven-distributed dataset. To prove that, we compared the model performance of our four-step model with the prediction performance of simulations using only the RF model and another decision-tree-based ensemble machine learning algorithm called XGBoost (Chen and Guestrin, 2016). The results are listed in Table S2. Compared to the RF model, our four-step model has a lower MAE by 15% and 19% for the winter-spring and summer fire season, respectively. Compared to the XGBoost model, the MAE from our four-step model is 11% and 15% lower for the two fire seasons. In addition, the distribution of percentiles is more uniform than the distribution of the burned area, as shown in Figure S2 and the skewness value. Details about calculation of skewness are described in Supporting Information. Larger positive skewness value indicates more highly right-skewed distribution. The skewness of burned area is 37.4 and 33.8 for the winter-spring and summer fire season while the skewness of percentiles is 0.7 and 0.96, showing that the strategy of the four-step model can effectively reduce unevenness of the distribution.

In addition to the grid-scale statistics, we evaluated the model performance at the large-domain scale by adding up all the grid-level predictions to obtain the total burned area of the study domain by months. Figure 5 shows the time series of the predicted total burned area over South Central US in comparison to the observed ones for the two fire seasons. The domain-scale prediction explains 50% and 79% of the month-to-month variability of burned area for the winter-spring and summer fire season, respectively. MAE of the monthly burned area across the whole domain is 251.3 km^2 for the winter-spring fire season and 100.7 km^2 for the summer fire season. As shown in Table S1, the prediction accuracy of our model in terms of R^2 is equivalent to or better than most of the published studies on the ecoregion scale or country scale.

5. Contributions of environmental factors to predicted wildfire burned area

5.1 Individual variable importance at grid scale

Before discussing the environmental controls on wildfire burned area across the study domain, it is useful to understand the dominant factors controlling the burned area at the grid scale. One advantage of the random forest approach is that it provides the variable importance metrics that can measure the power of predictor variables in the prediction. Figure 6 shows the top 14 predictors ranked by %IncMSE to illustrate the intricate relationships between fires, weather, climate, and fuel. The top 14 variables were chosen because they represent the top quarter (25%) of selected predictor variables. In addition, a sensitivity test shows that the largest drop in the %IncMSE occurs around the 15th variable ranked by importance, as shown in Table S4. To ensure the reliability of the inferred importance of predicted factors, we conducted 50 times 10-fold cross-

validation by randomizing the order of all the data each time. Figure S6 shows the distributions of %IncMSE for each variable ranked by the median %IncMSE. Even though the numerical values of feature importance vary in different runs, the variable ranks by median values stay the same, indicating the robustness of the feature importance identified by the RF model.

For both fire seasons, RH anomaly is the most important predictor of wildfire burned area at the grid-scale (Figure 6). This finding broadly supports past studies that highlighted the importance of RH on burned area (Riley et al., 2013; Ruthrof et al., 2016). Yet, our model particularly reveals the response of fire burned area to the changes in RH anomaly, which is a climate variable as opposed to a weather variable. RH anomaly indicates the changes of the fire-season RH relative to its historical climatology and it ranks higher than the actual value of the fire-season RH in the variable importance metrics.

While both fire season have RH as the top driver of burned area, notable differences are found for the relative importance of other variables between the two fire seasons. For the summer fire season, temperature anomaly and maximum temperature anomaly are other two climatic factors besides RH anomaly that are included in the top 14 variables. While RH anomaly and temperature anomaly are expected to correlate to some extent, their correlation is more negative in the summer fire season (r= -0.7) than in the spring fire season (r= -0.2). This highlights the importance of the stronger combined effects of RH and temperature anomalies on burned area during summer.

For the winter-spring fire season specifically, the long-term averages of monthly total precipitation and monthly means of daily precipitation (apcp_avg and asum avg) are identified as the key climate variables (Figure 6a). These two variables represent the precipitation normal, indicating the amount of available moisture that could affect fuel distributions and tendency of fire activities (Keyser and Westerling, 2017; Westerling and Bryant, 2008). The averaged SPEI of the preceding 4 months is the second most important variables and the highest-ranked weather variables, which is even more important than the SPEI during the fire season. The averaged SPEI of the preceding 3 months and 5 months are also included in the top 14 variables. The 3-5 months' time lag coincidentally corresponds to the interval between the two fire seasons. Thus, our results indicate that wildfire burned area in this season is highly dependent on the pre-fire-season drought conditions, which is in agreement with prior studies (Scott and Burgan., 2005; Riley et al., 2013; Turco et al., 2017). The variable importance by the RF is supported by the partial dependence plot which shows the marginal effect of a variable on the prediction performance (Friedman, 2001). Figure S7 shows the partial dependence plots for the burned area model and the top two variables of RH anomaly and mean SPEI of the preceding 4 months for the winter-spring fire season. For these two variables, there is a significant drop of fitted burned area when RH anomaly is larger than -1 and mean SPEI of the preceding 4 months larger than -0.6, demonstrating the large sensitivity of the predicted burned area to the top ranked variables. Interestingly, the average of LAI and sum of neighboring LAI for months *t-1* to *t-6* are the only fuel variables that are selected among the top 14 variables in the winter-spring fire season (Figure 6). Although these two variables rank below others among the top 14 variables, they are the fifth and sixth most important variables when excluding the fixed variables. Thus, when considering the importance of the time-varying variables, we can infer that fuel abundance together with drought conditions in the pre-fire-season determines the amount of dry fuel, which likely exerts the primary controls of the burned area during the winter-spring fire season. For the summer fire season, important weather variables include the average of monthly accumulated

precipitation of the preceding one month and the mean SPEI of the preceding one month, two months, and three months (Figure 6b). These variables are known to affect fire burned area by influencing fuel moisture. Consistently, fuel moisture as represented by soil moisture is identified as the only fuel variable among the top 14 variables in the summer fire season. These results suggest that fuel drying during the summer fire season driven by both increasing temperature and pre-fire season drought conditions is the pivotal process determining wildfire burned area in the summer. Similar to our findings, rising summer temperature under climate change was found to cause fast fuel dryness, which increased fire activity in the western US (Williams et al., 2013; Holden et al., 2018).

Overall, the analysis of variable importance reveals some important differences of the wildfire development between the two fire seasons and shows semi-quantitatively that drought conditions in the preceding months (3-5 months for the spring fire season and 1-3 months for the summer fire season) may be more important than within-season conditions. Furthermore, we demonstrate that the effect of climate variability on fire burned area is consequential and even more influential than concurrent fire weather. This aspect has not been well documented or quantified in past studies for the South Central US, partly due to a lack of long-term observations of wildfires over this region. Although we did not use long-term wildfire data (only 14-years of data used), with the 10-fold cross validation approach, the training dataset contains around 16277 samples for each fold. Such a large sample size is enough to capture the variability in wildfire activity and its response to recent decadal climate if we assume wildfire relationships with the environmental factors contain certain uniqueness for each individual grid.

5.2 Relative importance of environmental controls at large scale

The variable importance metrics presented in the previous section reveal the relative importance of individual predictors. As mentioned before, these predictors were purposely selected from four broadly defined categories of environmental controls on wildfire burned area, namely climate, weather, fuel, and fixed-geospatial. Here the climate category includes only variables of climate anomalies. The weather and fuel category are comprised of both fire-season and antecedent weather and fuel conditions, respectively. The fixed geospatial category includes all the variables that do not change with time, including land types, ecoregion types, population, and 22-year means and standard deviations of meteorological variables (i.e. climate normals). Given that variables within the same category may work in conjunction to create conditions conducive to wildfires, in this section we examine the composite influence of predictors by category and quantify the contributions of these environmental controls to wildfire burned area. To do so, the prediction model developed from Section 3 was used to decompose the effect of different environmental controls across our study domain by perturbing all the variables belonging to one category at a time. The details of the decomposition method were described in the supplementary information.

Figure S8 shows the time series of the burned area contributed by different environmental controls for the two fire seasons. The results show that the weather, fuel, climate, and fixed effects all tend to increase burned area while the interaction effect acts to reduce burned area, in particular for the large burn events (e.g. July 2011 in the summer fire season). As the number of variables in each environmental control category is different, we first normalized the absolute contribution of one environmental control by the number of variables in that category and then compared each category's contribution in scaled

absolute percentage, which is defined as normalized absolute contribution of one environmental control divided by the summation of normalized absolute contributions over all the categories. The scaled absolute percentage represents the average contribution from all the variables in one environmental category. Figure S9 shows the time series of the scaled absolute percentage by each category. For both fire seasons, on average, the climate and fixed categories have larger contributions to the burned area than other categories, although their relative importance varies by time. Figure 7 and Table S5 present the mean effect of the environmental controls where the scaled absolute percentage of each category of environmental controls is averaged over the whole study periods. Figure 7 clearly shows that the climate category on average has the largest contribution to burned area for both fire seasons, with the mean scaled absolute contribution of 33% and 35% for the winter-spring and summer fire season, respectively. This suggests climate variability is a significant factor to explain wildfire burned area over our study domain. This result is consistent with previous studies that demonstrated the significant contribution of changing climate to the total burned area of ecoregions or countries (Littell et al., 2009; Swetnam and Anderson, 2008; Yue et al., 2013). For example, increasing temperature and earlier spring snowmelt due to climate change are highly associated with increased large wildfire activity in the western US (Westerling et al., 2006). Another study showed that fire-year climate variables such as average spring temperature are predictive variables that could improve the predicting probability of high severity fires in the western US (Keyser and Westerling, 2017). Additionally, the fixed effect that comprises the geospatial variables and past climatology is ranked as the second most important control (Figure 7). This is consistent with the findings of Keyser and Westerling (2017), which revealed the importance of long-term climate normals in controlling large fire occurrences in the western US.

Comparing the effects of the environmental controls between the two fire seasons, we found the fuel effect is significantly more important in the winter-spring fire season, while weather and climate effects are more substantial in the summer fire season. This can probably be explained by the different characteristics of the two fire seasons. As biomass growth is relatively limited in the winter-spring fire season, the effect of fuel (mainly from vegetation in pre-fire growing season) is likely the limiting factor for wildfires in the winter-spring fire season. On the other hand, vegetation is relatively sufficient during the summer growing fire season and thus fuel abundance would not be a constraint of wildfires. Yet, fire weather that determines fuel moisture is a substantial factor in the summer fire season (Figure 7).

The above analysis represents the relative importance of the environmental controls at the large-domain scale. At the grid scale, we calculated the average of variable importance (%IncMSE) from RF (section 3.1.1) of each category and used the category-averaged variable importance to represent the relative importance at the grid-scale (Table S6). Climate variables are found to have the largest importance in controlling burned area at the grid scale for the two fire seasons, with the mean %IncMSE of 12.09 and 19.18 for the winter-spring and summer fire season, respectively. This is consistent with the results presented for the large-domain scale. Fuel effect outweighs weather effect on the grid scale in the winter-spring fire season, while weather effect is more important in the summer fire season, both consistent with the aforementioned analysis based on the large-scale domain (Table S6). However, the fixed effect estimated at the grid-scale is less important than at the large-scale domain (Table S6) and this is partly due to how these variables are coded in the model. Fixed variables consist of past

climatology and geospatial variables (i.e. land use, ecoregion, and population). The geospatial variables, except population, were encoded as categorical variables in the prediction model. For example, forest ecoregion is coded as 0 or 1 for a given grid, with 0 representing non-forest and 1 representing a forest. For such encoding method, each categorical variable (e.g. forest v.s. non-forest) tends to have a smaller relative importance score, compared to the relative importance score of other variables encoded by continuous values. As RF measures the effect of a specific split on the improvement in model performance and aggregates the improvement of all the splits with a specific variable, the fragmented scores for each category are likely smaller than the scores reflecting all of the categories. Therefore, for the relative importance at the grid level measured by RF, the effect of a single geospatial variable such as a land type on the burned area is trivial. When we averaged the relative importance of all the fixed variables including many small scores, the resulting average importance becomes still a small value.

6. Discussion and Conclusion

We presented a model integrating multiple machine learning methods to predict monthly burned area over South Central US at 0.5° x 0.5° grid cells. The prediction model is able to alleviate the issue of unevenly-distributed burned area and consequently improves the model capability of predicting large burned area at a finer spatial and temporal scale. The predicted burned area showed a good agreement with the observed burned area at both the grid and large-domain scale. At the grid scale, the classification component of the model achieves an AUC of 0.82 and 0.83 for the winter-spring and summer fire season, respectively. With respect to burned area prediction, a CV-R^2 of 0.42 and 0.40 is achieved for the winter-spring and summer fire season, respectively, which outperformed most past studies that predicted wildfire burned area at a coarser spatial and temporal scale. Our four-step model is able to predict the spatial patterns of the 14-year mean burned area, with a correlation coefficient between mean observed and predicted burned area of 0.82 and 0.80 for the winter-spring and summer fire season, respectively. Throughout the study period, more than 60% of the months have a spatial correlation larger than 0.5. When comparing the timeseries of observed and predicted burned area of each grid across the study domain, over 70% of the grids have a correlation coefficient larger than 0.5. At the large-domain scale, the prediction model can explain 50% and 79% of interannual variability of wildfire burned area for the winter-spring and summer fire season, respectively. The validation results demonstrate that the model has certain skills in predicting monthly burned area at both grid-scale and large-domain scale.

Although the model shows a better ability to predict monthly burned area at both grid-scale and large-domain scale than past studies of similar nature, it has several limitations. First, errors might be propagated through our serial model and lead to lower accuracy. For example, when the burned grids are predicted not to burn, low bias occurs because the burned grids are not able to enter step 3. Similarly, inclusion of unburned grids in step 3 will introduce a positive bias. Second, although for a single grid our four-step model can predict burned area greater than that grid had experienced before by learning from other grids, random forest or quantile regression forest cannot predict burned area greater than it observes before, i.e. the maximum

burned area of any of the available grids. For example, if the largest gridded burned area across the whole domain for the study period is 800 ha, the prediction for any single grid would never exceed 800 ha. Even though other methods such as MLR can predict burned area larger than it observes before, other uncertainties arise in extrapolation that are difficult to quantify (Amatulli et al., 2013; Mckenzie et al., 1996). For the machine learning methods such as RF, the model performance will keep improving as more data is included into the training set. Third, as machine learning models are data driven, data quality of different input datasets may introduce biases as the input datasets come from a wide variety of data sources and errors in one type of input data may cause sequential errors in the prediction. For instance, biases in the NARR meteorological data can further lead to incorrect fire-meteorology relationships learned by the model. Fourth, the present study focuses on the effects of environmental controls on burned area under present-day human management practices and human activity. As such, we do not examine the effects of time-varying socioeconomic factors on burned area, such as human actions that affect wildfires through ignition, suppression, or modifying fuel distribution (Andela et al., 2017; Bowman et al., 2011; Mann et al., 2016; Syphard et al., 2007). Given that human activity is one of the major controls on fire activity, future work is needed to better understand the role of human activity engaged with climate change and its implications for wildfire control. Finally, the pre-defined parameters that were used in the model, including the percentiles and subgroups, may induce uncertainties. To understand the related uncertainties, we switched the pre-defined percentiles but fixed the subgroups in the first sensitivity experiment (Table S7). In this experiment, the last three quantiles were changed to the median values between a new set of lower and upper bounds. The second experiment was conducted by changing the number of subgroups, their ranges, and the corresponding percentiles. Generally, changing pre-defined parameters has little effect on overall MAE for the two fire seasons but the MAE of large burned area becomes larger and the standard deviation of the predicted values becomes smaller. Thus, the pre-defined parameters most affect the spread of the predictions and the magnitudes of large burned areas. Despite this sensitivity, the prediction model with the chosen settings (i.e. percentiles and subgroups) is able to predict burned area at 0.5° x 0.5°-grid scale and achieve a higher prediction accuracy compared to prior studies.

The individual variable importance from the RF model was analyzed and discussed. For both fire seasons, RH anomaly followed by drought conditions in the preceding months (3-5 months for the winter-spring fire season and 1-3 months for the summer fire seasons) are the two top variables in predicting burned area at the grid scale. For the winter-spring fire season specifically, the average of LAI and sum of neighboring LAI of the preceding six months are the only two fuel variables that were identified in the top 14 variables and they ranked fifth and sixth when only considering time-varying variables. The findings suggest that fuel abundance together with drought conditions during the pre-fire season regulate the abundance of dry fuel, which is the primary control of fire burned area during the winter-spring seasons. For the summer fire season, temperature anomalies, the average of monthly accumulated precipitation of the preceding one month, and fire season soil moisture are important variables in predicting burned area. This suggests that temperature variability and pre-fire season drought can speed up fuel drying and lead to wildfires in the summer. The model highlights the effect of climate variability on burned area as well as the different environmental controls of burned area for the two fire seasons.

Besides the relative importance of individual predictors, we also analyzed the relative importance of the environmental controls by four categories - climate, weather, fuel, and fixed-geospatial - at both the grid and large-domain scale. The relative importance of these factors is generally consistent at the two scales. The climate variable on average has the largest contribution to burned area for both fire seasons, with the mean scaled absolute contribution of 33% and 35 % to the burned area at the large-domain scale for the winter-spring and summer fire season, respectively. For the winter-spring fire season, the fuel variable on average has larger importance compared to the weather variable; while for the summer fire season, the weather variable is more dominant than the fuel variable. The difference in the relative importance of the environmental controls between the large-domain scale and grid scale mainly lies in the predominance of the fixed effect. The fixed effect is ranked as the second most important control at the large-domain scale, but it is not as important at the grid scale.

The top ranking of predictor variables representing climate variability inferred by our prediction model reinforces the importance of regional climate variability as the key driver for wildfires that have been revealed by past studies for other regions, yet our study is among the first to explicitly demonstrate such importance for the South Central US. For this region, we further revealed drought conditions in the preceding 3-5 months of a fire season as an important predictor for wildfire burned area, which could be valuable for fire management and fire prediction in the future. While the relative importance of environmental controls is largely consistent between the large-domain scale (~700 km x 700 km) and the grid scale (~50 km x 50 km), the relative importance of predictors at the finer scale can be useful to better understand the environmental controls of wildfire across different spatial scales. Our analysis at different spatial scales will help estimate how the relationship between wildfire and environmental controls will change as a function of spatial scales, which could be used to improve wildfire modeling and prediction in different models.

Code availability. Model code is available upon request to the first author

Data availability. All dataset used in this study are publicly accessible online at https://dataverse.harvard.edu/dataset.xhtml?persistentId=doi%3A10.7910%2FDVN%2FLRPDAA

Author contributions. SW and YW conceived the research idea. SW wrote the initial draft of the paper, performed the analyses, and model development. All authors contributed to the interpretation of the results and the preparation of the manuscript.

Competing interests. The authors declare that they have no conflict of interest.

Acknowledgements. This work was funded in part with funds from an AI for Earth grant from Microsoft and from the State of Texas as part of the program of the Texas Air Research Center (grant number: 117UHH0175A). The contents do not necessarily reflect the views and policies of the sponsor nor does the mention of trade names or commercial products constitute endorsement or recommendation for use.

References

Amatulli, G., Camia, A. and San-Miguel-Ayanz, J.: Estimating future burned areas under changing climate in the EU-Mediterranean countries, Science of The Total Environment, 450–451, 209–222, doi:10.1016/j.scitotenv.2013.02.014, 2013.

An, H., Gan, J. and Cho, S. J.: Assessing Climate Change Impacts on Wildfire Risk in the United States, Forests, 6(9), 3197–3211, doi:10.3390/f6093197, 2015.

Andela, N., Morton, D. C., Giglio, L., Chen, Y., Werf, G. R. van der, Kasibhatla, P. S., DeFries, R. S., Collatz, G. J., Hantson, S., Kloster, S., Bachelet, D., Forrest, M., Lasslop, G., Mangeon, S., Melton, J. R., Yue, C. and Randerson, J. T.: A human-driven decline in global burned area, Science, 356(6345), 1356–1362, doi:10.1126/science.aal4108, 2017.

Baboo, S. and Devi, R.: An Analysis of Different Resampling Methods in Coimbatore, District, Global Journal of Computer Science and Technology, 10(15), 61–66, 2010.

Balshi, M. S., McGUIRE, A. D., Duffy, P., Flannigan, M., Walsh, J. and Melillo, J.: Assessing the response of area burned to changing climate in western boreal North America using a Multivariate Adaptive Regression Splines (MARS) approach, Global Change Biology, 15(3), 578–600, doi:10.1111/j.1365-2486.2008.01679.x, 2009.

Barbero, R., Abatzoglou, J. T., Larkin, N. K., Kolden, C. A. and Stocks, B.: Climate change presents increased potential for very large fires in the contiguous United States, Int. J. Wildland Fire, 24(7), 892–899, doi:10.1071/WF15083, 2015.

Bedia, J., Herrera, S. and Gutiérrez, J. M.: Assessing the predictability of fire occurrence and area burned across phytoclimatic regions in Spain, Natural Hazards and Earth System Sciences, 14(1), 53–66, doi:https://doi.org/10.5194/nhess-14-53-2014, 2014.

Bowman, D. M. J. S., Balch, J. K., Artaxo, P., Bond, W. J., Carlson, J. M., Cochrane, M. A., D'Antonio, C. M., DeFries, R. S., Doyle, J. C., Harrison, S. P., Johnston, F. H., Keeley, J. E., Krawchuk, M. A., Kull, C. A., Marston, J. B., Moritz, M. A., Prentice, I. C., Roos, C. I., Scott, A. C., Swetnam, T. W., Werf, G. R. van der and Pyne, S. J.: Fire in the Earth System, Science, 324(5926), 481–484, doi:10.1126/science.1163886, 2009.

Bowman, D. M. J. S., Balch, J., Artaxo, P., Bond, W. J., Cochrane, M. A., D'Antonio, C. M., DeFries, R., Johnston, F. H., Keeley, J. E., Krawchuk, M. A., Kull, C. A., Mack, M., Moritz, M. A., Pyne, S., Roos, C. I., Scott, A. C., Sodhi, N. S. and Swetnam, T. W.: The human dimension of fire regimes on Earth, Journal of Biogeography, 38(12), 2223–2236, doi:10.1111/j.1365-2699.2011.02595.x, 2011.

Camia, A., and Amatulli, G.: Weather Factors and Fire Danger in the Mediterranean, Earth Observation of Wildland Fires in Mediterranean Ecosystems, 71–82, doi:10.1007/978-3-642-01754-4_6, 2010.

Carvalho, Flannigan, M., Logan, Miranda, A. and Borrego, C.: Fire activity in Portugal and its relationship to weather and the Canadian Fire Weather Index System, International Journal of Wildland Fire, 17, 328–338, doi:10.1071/WF07014, 2008.

Chen, T. and Guestrin, C.: XGBoost: A Scalable Tree Boosting System, in Proceedings of the 22nd ACM SIGKDD International Conference on Knowledge Discovery and Data Mining, pp. 785–794, Association for Computing Machinery, San Francisco, California, USA., 2016.

Chen, Y., Morton, D. C., Andela, N., Giglio, L. and Randerson, J. T.: How much global burned area can be forecast on seasonal time scales using sea surface temperatures?, Environ. Res. Lett., 11(4), 045001, doi:10.1088/1748-9326/11/4/045001, 2016.

Dormann, C. F., Elith, J., Bacher, S., Buchmann, C., Carl, G., Carré, G., Marquéz, J. R. G., Gruber, B., Lafourcade, B., Leitão,

P. J., Münkemüller, T., McClean, C., Osborne, P. E., Reineking, B., Schröder, B., Skidmore, A. K., Zurell, D. and Lautenbach, S.: Collinearity: a review of methods to deal with it and a simulation study evaluating their performance, Ecography, 36(1), 27–46, doi:10.1111/j.1600-0587.2012.07348.x, 2013.

Duane, A., Kelly, L., Gijohann, K., Batllori, E., McCarthy, M. and Brotons, L.: Disentangling the Influence of Past Fires on Subsequent Fires in Mediterranean Landscapes, Ecosystems, 22(6), 1338-1351, doi:10.1007/s10021-019-00340-6, 2019.

Fang, L., Yang, J., Zu, J., Li, G. and Zhang, J.: Quantifying influences and relative importance of fire weather, topography, and vegetation on fire size and fire severity in a Chinese boreal forest landscape, Forest Ecology and Management, 356, 2–12, doi:10.1016/j.foreco.2015.01.011, 2015.

Fann, N., Alman, B., Broome, R. A., Morgan, G. G., Johnston, F. H., Pouliot, G. and Rappold, A. G.: The health impacts and economic value of wildland fire episodes in the U.S.: 2008-2012, Sci. Total Environ., 610–611, 802–809, doi:10.1016/j.scitotenv.2017.08.024, 2018.

Fernandes, P. M., Monteiro-Henriques, T., Guiomar, N., Loureiro, C. and Barros, A. M. G.: Bottom-Up Variables Govern Large-Fire Size in Portugal, Ecosystems, 19(8), 1362–1375, doi:10.1007/s10021-016-0010-2, 2016.

Flannigan, M. D., Logan, K. A., Amiro, B. D., Skinner, W. R., and Stocks, B. J.: Future area burned in Canada, Climate Change, 72(1), 1–16, doi: 10.1007/s10584-005-5935-y, 2005.

Fréjaville, T. and Curt, T.: Seasonal changes in the human alteration of fire regimes beyond the climate forcing, Environ. Res. Lett., 12(3), 035006, doi:10.1088/1748-9326/aa5d23, 2017.

Friedman, J. H.: Greedy Function Approximation: A Gradient Boosting Machine, The Annals of Statistics, 29(5), 1189–1232, 2001.

Heyerdahl, E. K., McKenzie, D., Daniels, L. D., Hessl, A. E., Littell, J. S. and Mantua, N. J.: Climate drivers of regionally synchronous fires in the inland northwest (1651-1900), International Journal of Wildland Fire. 17: 40-49., 2008.

Holden, Z. A., Swanson, A., Luce, C. H., Jolly, W. M., Maneta, M., Oyler, J. W., Warren, D. A., Parsons, R. and Affleck, D.: Decreasing fire season precipitation increased recent western US forest wildfire activity, PNAS, 115(36), E8349–E8357, doi:10.1073/pnas.1802316115, 2018.

Jaffe, D., Hafner, W., Chand, D., Westerling, A. and Spracklen, D.: Interannual Variations in PM2.5 due to Wildfires in the Western United States, Environ. Sci. Technol., 42(8), 2812–2818, doi:10.1021/es702755v, 2008.

Keane, R. E., Reinhardt, E. D., Scott, J., Gray, K. and Reardon, J.: Estimating forest canopy bulk density using six indirect methods, Canadian Journal of Forest Research, 35(3), 724–739, doi:10.1139/x04-213, 2005.

Keyser, A. and Westerling, A. L.: Climate drives inter-annual variability in probability of high severity fire occurrence in the western United States, Environ. Res. Lett., 12(6), 065003, doi:10.1088/1748-9326/aa6b10, 2017.

Kirchmeier-Young, M. C., Gillett, N. P., Zwiers, F. W., Cannon, A. J. and Anslow, F. S.: Attribution of the Influence of Human-Induced Climate Change on an Extreme Fire Season, Earth's Future, 7(1), 2-10, doi:10.1029/2018EF001050, 2018.

Krawczyk, B.: Learning from imbalanced data: open challenges and future directions, Prog Artif Intell, 5(4), 221–232, doi:10.1007/s13748-016-0094-0, 2016.

Krueger, E. S., Ochsner, T. E., Carlson, J. D., Engle, D. M., Twidwell, D. and Fuhlendorf, S. D.: Concurrent and antecedent

soil moisture relate positively or negatively to probability of large wildfires depending on season, Int. J. Wildland Fire, 25(6), 657–668, doi:10.1071/WF15104, 2016.

Liaw, A. and Wiener, M.: Classification and Regression by randomForest, R News, 2, 18-22, 2002.

Littell, J. S., McKenzie, D., Peterson, D. L. and Westerling, A. L.: Climate and wildfire area burned in western U.S. ecoprovinces, 1916–2003, Ecological Applications, 19(4), 1003–1021, doi:10.1890/07-1183.1, 2009.

Liu, Y., L. Goodrick, S. and A. Stanturf, J.: Future U.S. wildfire potential trends projected using a dynamically downscaled climate change scenario, Forest Ecology and Management, 294, 120–135, doi:10.1016/j.foreco.2012.06.049, 2013.

Liu, Z. and Wimberly, M. C.: Climatic and Landscape Influences on Fire Regimes from 1984 to 2010 in the Western United States, PLOS ONE, 10(10), e0140839, doi:10.1371/journal.pone.0140839, 2015.

Long, D., Scanlon, B. R., Longuevergne, L., Sun, A. Y., Fernando, D. N. and Save, H.: GRACE satellite monitoring of large depletion in water storage in response to the 2011 drought in Texas, Geophysical Research Letters, 40(13), 3395–3401, doi:10.1002/grl.50655, 2013.

Mann, M. L., Batllori, E., Moritz, M. A., Waller, E. K., Berck, P., Flint, A. L., Flint, L. E. and Dolfi, E.: Incorporating Anthropogenic Influences into Fire Probability Models: Effects of Human Activity and Climate Change on Fire Activity in California, PLOS ONE, 11(4), e0153589, doi:10.1371/journal.pone.0153589, 2016.

Mckenzie, D., Peterson, D. L. and Alvarado, E.: Extrapolation Problems in Modeling Fire Effects at Large Spatial Scales: a Review, Int. J. Wildland Fire, 6(4), 165–176, doi:10.1071/wf9960165, 1996.

Meinshausen, N.: Quantile Regression Forests, Journal of Machine Learning Research, 7(Jun), 983–999, 2006.

Metz, C. E.: Basic principles of ROC analysis, Semin Nucl Med, 8(4), 283–298, doi:10.1016/s0001-2998(78)80014-2, 1978.

Morgan, P., Heyerdahl, E. K. and Gibson, C. E.: Multi-season climate synchronized forest fires throughout the 20th century, Northern Rockies, USA, Ecology. 89(3): 717-728, 2008.

Nielsen-Gammon, J. W.: The 2011 Texas Drought, Texas Water Journal, 3(1), 59–95, 2012.

Nunes, M. C. S., Vasconcelos, M. J., Pereira, J. M. C., Dasgupta, N., Alldredge, R. J. and Rego, F. C.: Land Cover Type and Fire in Portugal: Do Fires Burn Land Cover Selectively?, Landscape Ecol, 20(6), 661–673, doi:10.1007/s10980-005-0070-8, 2005.

Parisien, M.-A., Parks, S. A., Krawchuk, M. A., Flannigan, M. D., Bowman, L. M. and Moritz, M. A.: Scale-dependent controls on the area burned in the boreal forest of Canada, 1980-2005, Ecol Appl, 21(3), 789–805, doi:10.1890/10-0326.1, 2011.

Parks, S. A., Parisien, M.-A. and Miller, C.: Spatial bottom-up controls on fire likelihood vary across western North America, Ecosphere. 3(1): Article 12., doi:10.1890/ES11-00298.1, 2012.

Pausas, J. G. and Keeley, J. E.: A Burning Story: The Role of Fire in the History of Life, BioScience, 59(7), 593–601, doi:10.1525/bio.2009.59.7.10, 2009.

Pellegrini, A. F. A., Anderegg, W. R. L., Paine, C. E. T., Hoffmann, W. A., Kartzinel, T., Rabin, S. S., Sheil, D., Franco, A. C. and Pacala, S. W.: Convergence of bark investment according to fire and climate structures ecosystem vulnerability to future change, Ecology Letters, 20(3), 307–316, doi:10.1111/ele.12725, 2017.

Peters, D. P. C., Pielke, R. A., Bestelmeyer, B. T., Allen, C. D., Munson-McGee, S. and Havstad, K. M.: Cross-scale interactions, nonlinearities, and forecasting catastrophic events, PNAS, 101(42), 15130–15135, doi:10.1073/pnas.0403822101, 2004.

Riley, K. L., Abatzoglou, J. T., Grenfell, I. C., Klene, A. E. and Heinsch, F. A.: The relationship of large fire occurrence with drought and fire danger indices in the western USA, 1984–2008: the role of temporal scale, International Journal of Wildland Fire, 22(7), 894, doi:10.1071/WF12149, 2013.

Ruthrof, K. X., Fontaine, J. B., Matusick, G., Breshears, D. D., Law, D. J., Powell, S. and Hardy, G.: How drought-induced forest die-off alters microclimate and increases fuel loadings and fire potentials, Int. J. Wildland Fire, 25(8), 819–830, doi:10.1071/WF15028, 2016.

Scott, J. H. and Burgan, R. E.: Standard fire behavior fuel models: a comprehensive set for use with Rothermel's surface fire spread model, Gen. Tech. Rep. RMRS-GTR-153. Fort Collins, CO: U.S. Department of Agriculture, Forest Service, Rocky Mountain Research Station. 72 p., 153, doi:10.2737/RMRS-GTR-153, 2005.

Short, K. C.: A spatial database of wildfires in the United States, 1992-2011, Earth System Science Data, 6, 1–27, doi:10.5194/essd-6-1-2014, 2014.

Short, K. C.: Spatial wildfire occurrence data for the United States, 1992-2015, Forest Service Research Data Archive (4th Edition), doi:10.2737/RDS-2013-0009.4, 2017.

Slocum, M. G., Beckage, B., Platt, W. J., Orzell, S. L. and Taylor, W.: Effect of Climate on Wildfire Size: A Cross-Scale Analysis, Ecosystems, 13(6), 828–840, doi:10.1007/s10021-010-9357-y, 2010.

Sousa, P. M., Trigo, R. M. and Pereira, M. G.: Different approaches to model future burnt area in the Iberian Peninsula, Agricultural and Forest Meteorology, 202, 11–25, doi: 10.1016/j.agrformet.2014.11.018, 2015.

Spracklen, D. V., Mickley, L. J., Logan, J. A., Hudman, R. C., Yevich, R., Flannigan, M. D. and Westerling, A. L.: Impacts of climate change from 2000 to 2050 on wildfire activity and carbonaceous aerosol concentrations in the western United States, Journal of Geophysical Research: Atmospheres, 114(D20), doi: 10.1029/2008JD010966, 2009.

Steele-Feldman, A., Reinhardt, E. and Parsons, R. A.: Fuels Management-How to Measure Success: Conference Proceedings, USDA Forest Proceedings, 283–291, 2006.

Steel, Z. L., Safford, H. D. and Viers, J. H.: The fire frequency-severity relationship and the legacy of fire suppression in California forests, Ecosphere, 6(1), 1–23, doi:10.1890/ES14-00224.1, 2015.

Swetnam, T. W. and Anderson, R. S.: Fire Climatology in the western United States: introduction to special issue, Int. J. Wildland Fire, 17(1), 1–7, doi:10.1071/WF08016, 2008.

Syphard, A. D., Radeloff, V. C., Keeley, J. E., Hawbaker, T. J., Clayton, M. K., Stewart, S. I. and Hammer, R. B.: Human Influence on California Fire Regimes, Ecological Applications, 17(5), 1388–1402, doi:10.1890/06-1128.1, 2007.

Turco, M., Hardenberg, J. von, AghaKouchak, A., Llasat, M. C., Provenzale, A. and Trigo, R. M.: On the key role of droughts in the dynamics of summer fires in Mediterranean Europe, Scientific Reports, 7(81), doi:10.1038/s41598-017-00116-9, 2017.

Urbieta, I. R., Zavala, G., Bedia, J., Gutierrez, J. M., San Miguel-Ayanz, J., Camia, A., Keeley, J. E. and Moreno, J. M.: Fire activity as a function of fire–weather seasonal severity and antecedent climate across spatial scales in southern Europe and Pacific western USA, Environmental Research Letters, 10(11), doi:10.1088/1748-9326/10/11/114013, 2015.

Vicente-Serrano, S. M., Beguería, S. and López-Moreno, J. I.: A Multiscalar Drought Index Sensitive to Global Warming: The Standardized Precipitation Evapotranspiration Index, J. Climate, 23(7), 1696–1718, doi:10.1175/2009JCLI2909.1, 2009.

Wang, S.-C., Wang, Y., Estes, M., Lei, R., Talbot, R., Zhu, L. and Hou, P.: Transport of Central American Fire Emissions to the U.S. Gulf Coast: Climatological Pathways and Impacts on Ozone and PM2.5, Journal of Geophysical Research: Atmospheres, 123(15), 8344–8361, doi:10.1029/2018JD028684, 2018.

Westerling, A. L.: Increasing western US forest wildfire activity: sensitivity to changes in the timing of spring, Philosophical Transactions of the Royal Society B: Biological Sciences, 371(1696), 20150178, doi:10.1098/rstb.2015.0178, 2016.

Westerling, A. L. and Bryant, B. P.: Climate change and wildfire in California, Climatic Change, 87(1), 231–249, doi:10.1007/s10584-007-9363-z, 2008.

Westerling, A. L., Turner, M. G., Smithwick, E. A. H., Romme, W. H. and Ryan, M. G.: Continued warming could transform Greater Yellowstone fire regimes by mid-21st century, Proceedings of the National Academy of Sciences, 108(32), 13165-13170, doi:10.1073/pnas.1110199108, 2011.

Westerling, A. L., Hidalgo, H. G., Cayan, D. R. and Swetnam, T. W.: Warming and Earlier Spring Increase Western U.S. Forest Wildfire Activity, Science, 313(5789), 940–943, doi:10.1126/science.1128834, 2006.

Williams, P. A., Allen, C. D., Macalady, A. K., Griffin, D., Woodhouse, C. A., Meko, D. M., Swetnam, T. W., Rauscher, S. A., Seager, R., Grissino-Mayer, H. D., Dean, J. S., Cook, E. R., Gangodagamage, C., Cai, M. and McDowell, N. G.: Temperature as a potent driver of regional forest drought stress and tree mortality, Nature Climate Change, 3(3), 292–297, doi:10.1038/nclimate1693, 2013.

Yue, X., Mickley, L. J., Logan, J. A. and Kaplan, J. O.: Ensemble projections of wildfire activity and carbonaceous aerosol concentrations over the western United States in the mid-21st century, Atmos Environ (1994), 77, 767–780, doi:10.1016/j.atmosenv.2013.06.003, 2013.

Yue, X., Mickley, L. J., Logan, J. A., Hudman, R. C., Martin, M. V. and Yantosca, R. M.: Impact of 2050 climate change on North American wildfire: consequences for ozone air quality, Atmospheric Chemistry and Physics, 15(17), 10033–10055, doi:https://doi.org/10.5194/acp-15-10033-2015, 2015.

Zhang, X., Kondragunta, S. and Roy, D. P.: Interannual variation in biomass burning and fire seasonality derived from geostationary satellite data across the contiguous United States from 1995 to 2011, Journal of Geophysical Research: Biogeosciences, 119(6), 1147–1162, doi:10.1002/2013JG002518, 2014.

Zubkova, M., Boschetti, L., Abatzoglou, J. T. and Giglio, L.: Changes in Fire Activity in Africa from 2002 to 2016 and Their Potential Drivers, Geophysical Research Letters, 46(13), 7643–7653, doi:10.1029/2019GL083469, 2019.

760 **Table 1.** Predictor variables that were used in the fire prediction models

Variables	Abbreviation	Categories	Temporal resolution	Spatial resolution	Data source
Weather variables					
Monthly mean surface temperature	temp	weather			
Monthly mean of daily precipitation	apcp	weather			
Monthly total precipitation	asum	weather			
Monthly mean surface relative humidity (%)	rhum	weather			
Monthly mean U-component of wind speed	U	weather	monthly	32 km	North American Regional Reanalysis (NARR)
Monthly mean V-component of wind speed	V	weather			
Monthly maximum temperature	tmax	weather			
Monthly minimum RH	rmin	weather			
Number of consecutive days without rainfall in a month	LargeConsec	weather			
1-month SPEI	SPEI	weather	1-month	0.5°	Global SPEI database
Fuel variables					
Monthly mean Leaf Area Index (LAI)	LAI	fuel	monthly	500 m	MODerate resolution Imaging Spectroradiometer (MODIS)
Monthly mean sum of neighboring LAI	convLAI	fuel	monthly	500 m	MODerate resolution Imaging Spectroradiometer (MODIS)
Monthly mean soil moisture at 0-10 cm	soil	fuel	monthly	0.125°	North American Land Data Assimilation System (NLDAS-2)
Geospatial and population variables					
Land types	land_	fix		30 m	National Land Cover Database (NLCD)
Ecoregion types	eco_	fix			U.S. Environmental Protection Agency (EPA)
Population density	pop	fix			U.S. Census 2010
Climate variables (over 1970-2000)					
Long-term average and standard deviation of monthly temperature	temp_avg; temp_sd	fix			

Long-term average and standard deviation of monthly mean of daily precipitation	apcp_avg; apcp_sd	fix			
Long-term average and standard deviation of monthly maximum temperature	tmax_avg; tmax_sd	fix			
Long-term average and standard deviation of monthly total precipitation	asum_avg; asum_sd	fix			
Climate anomalies of monthly mean temperature	temp_anomaly	climate	monthly	32 km	North American Regional Reanalysis (NARR)
Climate anomalies of monthly mean of daily precipitation	apcp_anomaly	climate			
Climate anomalies of monthly mean RH	rhum_anomaly	climate			
Climate anomalies of monthly maximum temperature	tmax_anomaly	climate			
Climate anomalies of monthly minimum RH	rmin_anomaly	climate			
Climate anomalies of monthly total precipitation	asum_anomaly	climate			
Lagged variables					
Winter-spring fire season					
The monthly mean of daily precipitation of months *t-1*	apcp_mean1m	weather	monthly	32 km	North American Regional Reanalysis (NARR)
The average SPEI of the months *t-1*, *t-1* to *t-2*, *t-1* to *t-3*, *t-1* to *t-4*, *t-1* to *t-5*, and *t-1* to *t-6*	SPEI_mean1m	weather	monthly	32 km	North American Regional Reanalysis (NARR)
The averages of LAI and sum of neighboring LAI for the months *t-1* to *t-6*	LAI_mean6m, convLAI_mean6m	fuel	monthly	500 m	MODerate resolution Imaging Spectroradiometer (MODIS)
Summer fire season					
The average of monthly mean of daily precipitation for months *t-1, t-1* to *t-2*	apcp_mean1m	weather	monthly	32 km	North American Regional Reanalysis (NARR)
The average of monthly mean temperature for months *t-1* and *t-1* to *t-2*	temp_mean1m	weather	monthly	32 km	North American Regional Reanalysis (NARR)
The average of SPEI of months *t-1*, *t-1* to *t-2*, and *t-1* to *t-3*	SPEI_mean1m	weather	1-month	0.5°	Global SPEI database

Table 2. Model performance at grid level for the two fire seasons.

Fire season	Evaluation Metrics							
	Accuracy	Recall	Precision	F1-score	AUC	R^2	RMSE (km^2)	MAE (km^2)
F1	0.74	0.88	0.73	0.79	0.82	0.42	8.37	1.13
F2	0.74	0.84	0.71	0.77	0.83	0.40	4.26	0.57

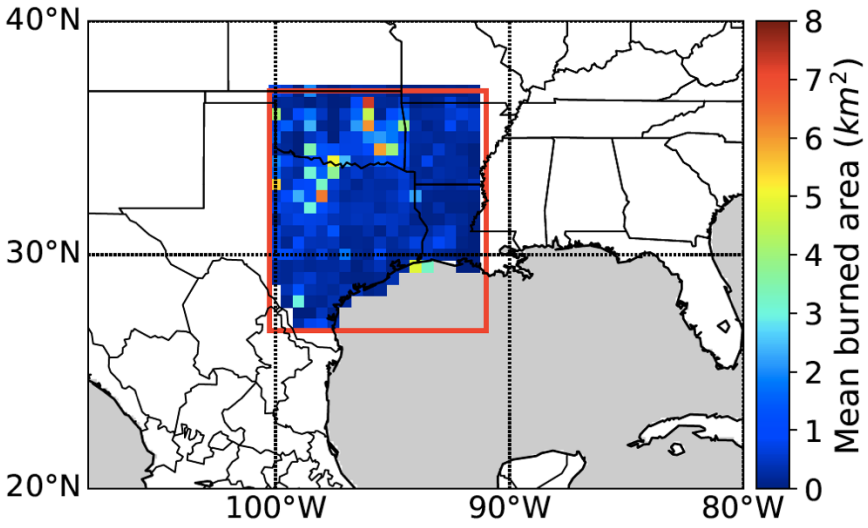

Figure 1. The colored grid boxes show the averaged burned area for the winter-spring and summer fire seasons during 2002-2015 from Fire Program Analysis Fire-Occurrence Database (FPA-FOD). The red box denotes the South Central US domain.

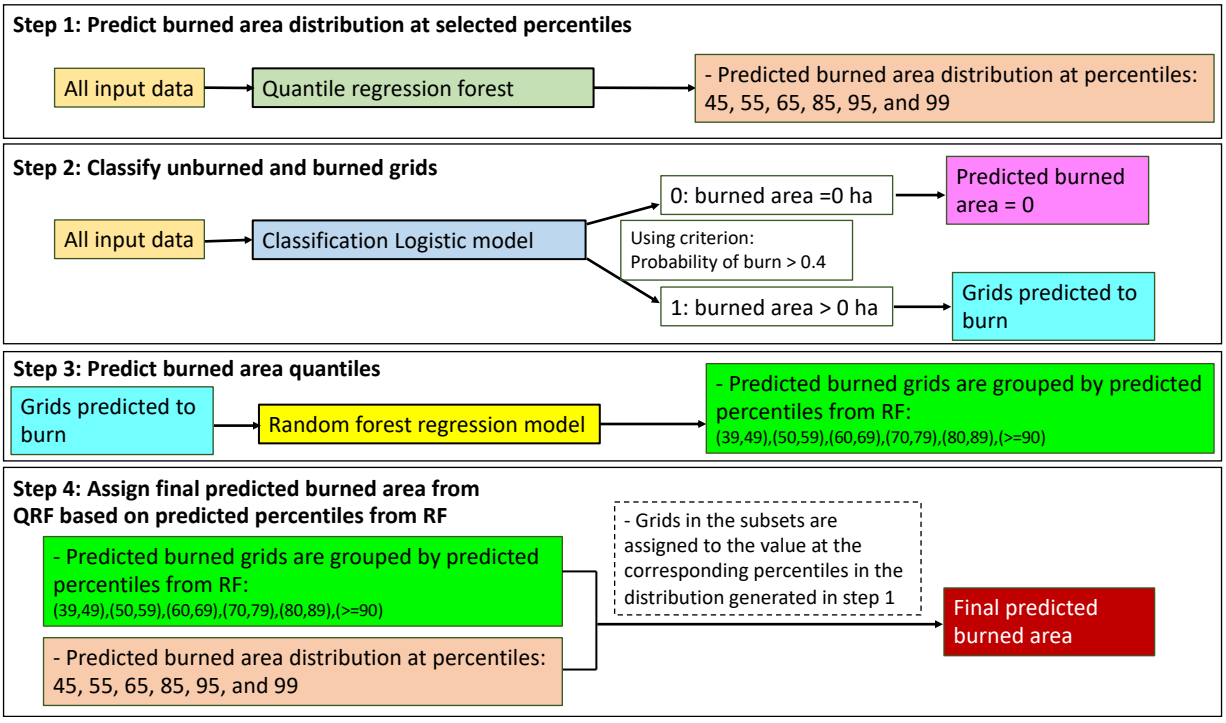

Figure 2. Illustration of the steps in the developed model. The model includes four steps and three machine learning algorithms, including a logistic model (dark blue) classifying a grid with non-zero burned area or not, a random forest model (yellow) predicting percentiles of burned area, and a quantile regression forest (dark green) predicting conditional burned area distributions.

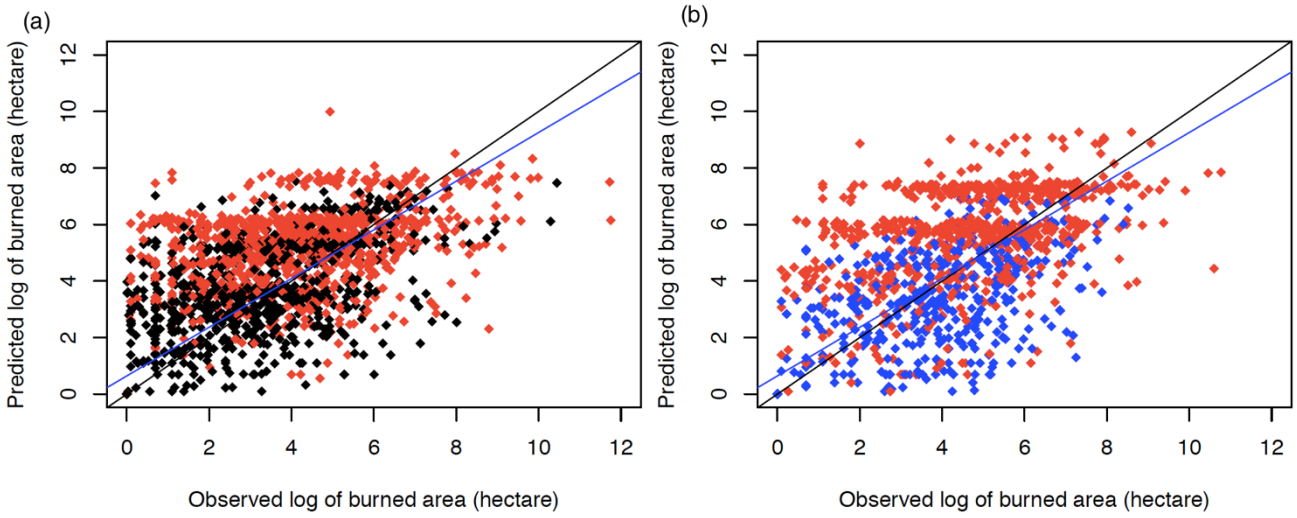

Figure 3. Comparison between log of observed and predicted burned area (hectare) for the (a) winter-spring and (b) summer fire season in selected years: 2011 (red, year of the largest burned area), 2008 (blue, year with burned area close to the 14-year mean of its season), and 2014 (black, year with burned area close to the 14-year mean of its season). The black line represents the line of unity and the blue line is a best fit to the data by linear regression.

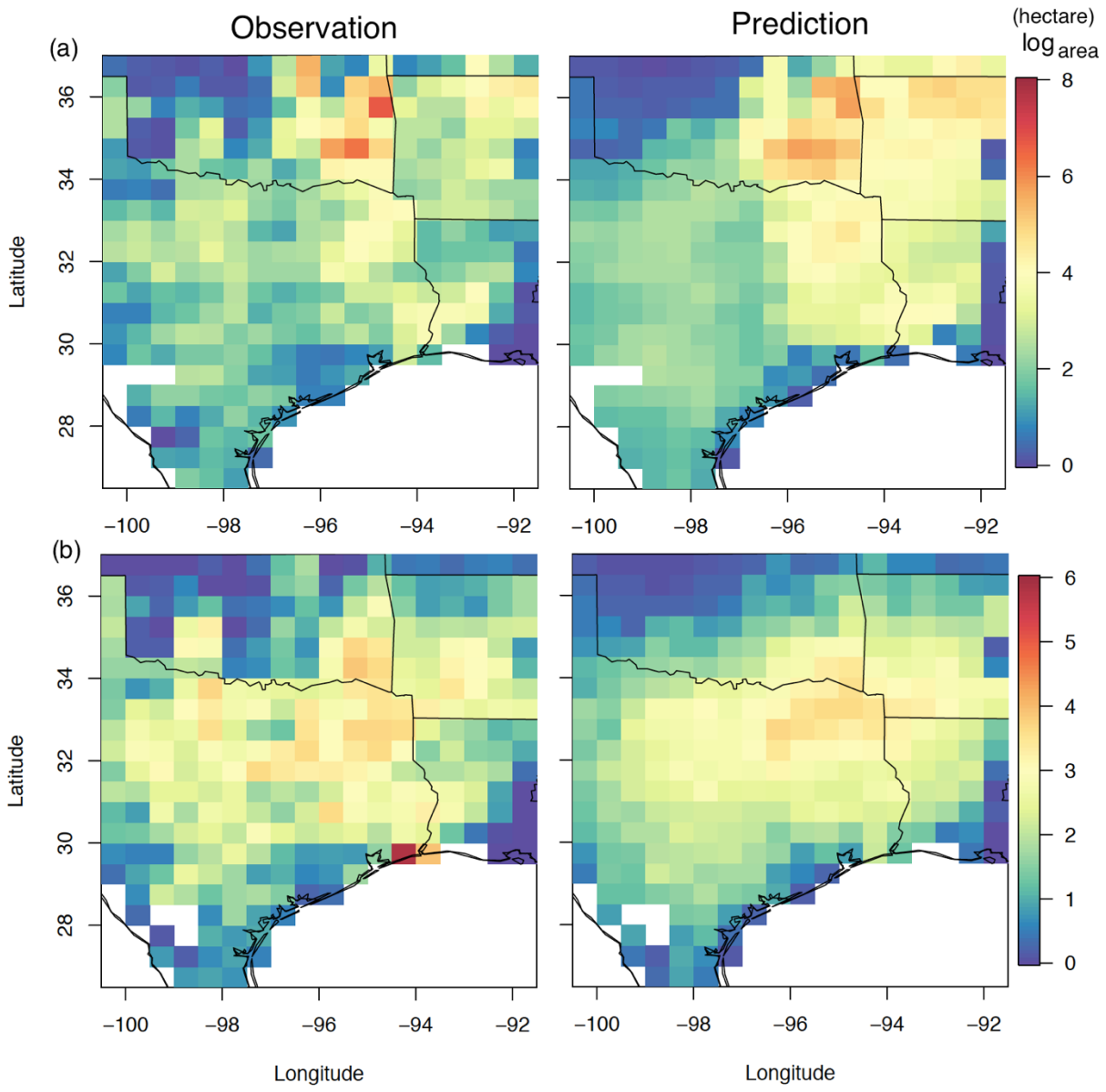

Figure 4. Map of monthly mean observed and predicted burned area averaged from 2002 to 2015 for the (a) winter-spring and (b) summer fire season.

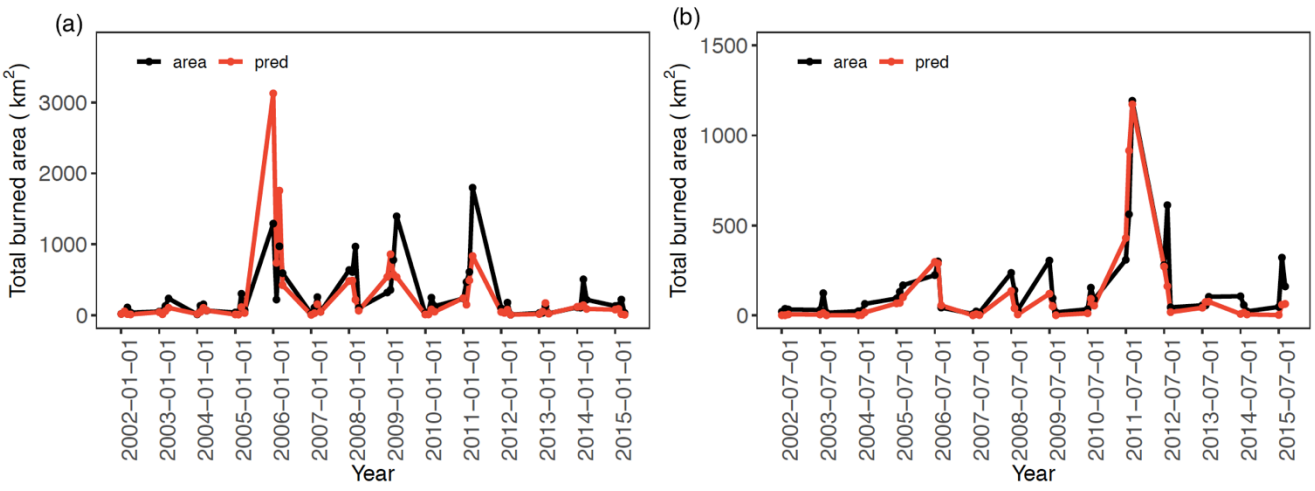

805 **Figure 5.** Timeseries of observed (black line) and predicted total burned area (red line) over South Central US for the (a) winter-spring and (b) summer fire season.

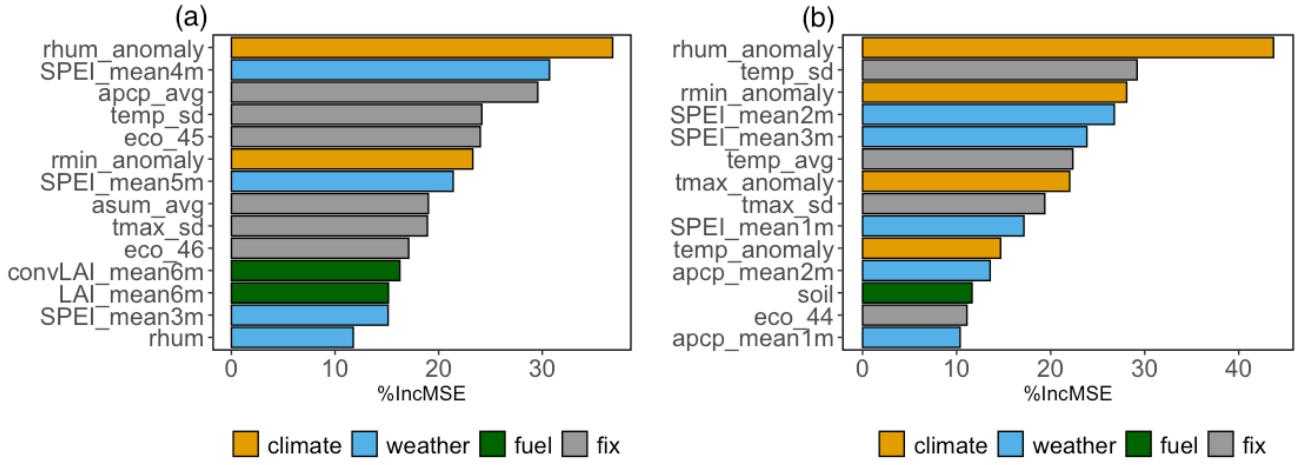

810

Figure 6. Relative importance of the top 14 variables presented by increase in mean square errors (%Inc.MSE) for (a) the winter-spring fire season (b) summer fire season.

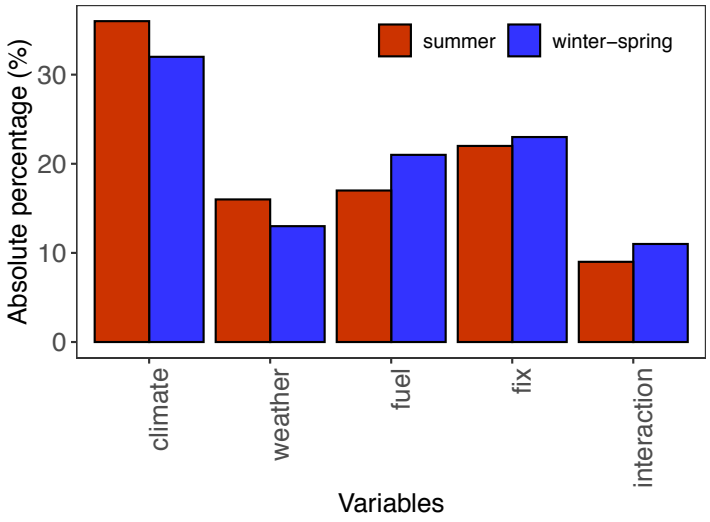

815

Figure 7. The mean scaled absolute percentage of the environmental controls for the winter-spring (blue) and summer fire season (red).

Supplement

Table S1. Studies using statistical methods to estimate burned area

Region	period	Method	Spatial domain	Spatial scale (estimated; km^2)	Temporal scale	R^2	Reference
Canada	1959-1997	MLR	Ecoregions	466x466~1123x1123	Monthly	36-64%	Flannigan et al. (2005)
Portugal	1980-2004	MLR	Portuguese districts	25x25~100x100	Monthly	43-80%	Carvalho et al. (2008)
Alaska and Canada	1960-2002	MARS	Alaska and western Canada	100x100~235x235	Annually	82%	Balshi et al. (2009)
EU-Mediterranean		MLR	European Mediterranean basin	1400x1400	Monthly	87%	Camia and Amatulli (2009)*
Western US	1916-2003	MLR [1]	Ecoregions	600x600~1000x1000	Annually	25-57%	Listtell et al. (2009)
Western US	1980-2004	MLR	Ecoregions	600x600~1000x1000	Annually	37-57%	Spracklen et al. (2009)
Western US	1972-1988; 1989-2005	MLR, RF [2]	NUTS3[4]	600x600~1000x1000	Annually	73%; 83%	Westerling et al. (2011)
EU-Mediterranean	1985-2004	MLR	Countries	300x300~1000x1000	Monthly	39-69%	Amatulli et al. (2013)
EU-Mediterranean	1985-2004	RF	Countries		Monthly	33-72%	Amatulli et al. (2013)
EU-Mediterranean	1985-2004	MARS [3]	Countries		Monthly	43-77%	Amatulli et al. (2013)
Spain	1990-2008	MARS	Phytoclimatic zones	25x25~100x100	Monthly	1-37%	Bedia et al. (2013)
Western US	1916-2004	MLR	Ecoregions	600x600~1000x1000	Annually	25-60%	Yue et al. (2013)
Western US	1916-2004	Parameterization	Ecoregions		Annually	1-69%	Yue et al. (2013)
North-eastern Spain	1983-2012	MLR	Catalonia	300x300	Annually	33%	Marcos et al. (2015)
Iberian Peninsula	1981-2005	MLR	Pyro-regions	200x200~700x700	Monthly	52-72%	Sousa et al. (2015)
EU-Mediterranean	1985-2011	MLR	EUMED [5]	2000x2000	Annually	60%	Urbieta et al. (2015)
Pacific western coast of USA	1985-2011	MLR	Oregon and California	1000x1000	Annually	37%	Urbieta et al. (2015)
British Columbia, Canada	1961-2010	MLR	Southern Cordillera	1400x1400	Annually	55%	Kirchmeier-Young et al. (2018)

Catalonia, Iberian Peninsula	1982-2015	MLR	Fire regime zones	80x80~150x150	Annually	57-91%	Duane et al. (2019)
South-Central US	2002-2015	Integration of RF, logistic regression, and QRF	Eastern Texas, Oklahoma, Louisiana, and Arkansas	700x700	Monthly	50% (winter-spring); 79% (summer)	This study

[1] MLR: Multiple Linear Regression; [2] RF: Random forest; [3] MARS: Multivariate adaptive regression Splines; [4] NUTS3: Nomenclature of Territorial Units at the third level [5] EUMED: burned area summation over Portugal, Spain, South France, Italy and Greece

*: focus on only large fires

Table S2. Comparison of MAE and skewness between the RF model and the developed model

Metrics	**Model developed in this study**	**RF alone**	**XGboost alone**
MAE (winter-spring)	1.13	1.34	1.26
Skewness (winter-spring) §	0.70 (percentiles)	37.40 (burned area)	37.40 (burned area)
MAE (summer)	0.57	0.70	0.67
Skewness (summer) §	0.96 (percentiles)	33.83 (burned area)	33.83 (burned area)

§: Skewness: The calculation of the skewness is described below in the section of calculation of skewness.

Table S3. Model performance at grid level for the selected years (excluding the misclassified grids)

Year/Fire season	Including misclassified grids			Excluding misclassified grids		
	R^2	RMSE (km^2)	MAE (km^2)	R^2	RMSE (km^2)	MAE (km^2)
2011 (combine winter-spring and summer)	0.30	11.04	3.38	0.42	21.06	5.25
2014 (winter-spring)	0.30	5.19	1.05	0.51	5.87	0.77
2008 (summer)	0.42	1.58	0.38	0.66	1.75	0.43

Table S4. The ratio of %IncMSE at variable ranked as X percentile (Y^{th}) to the %IncMSE at variable ranked as $(Y+1)^{th}$ for the three selected percentiles

	25^{th} percentile (Y=14)	50^{th} percentile (Y=29)	75^{th} percentile (Y=43)
Spring-winter	1.21	0.88	1.00
Summer	1.06	1.01	1.00

Table S5. The mean scaled absolute percentage of each effects for the two fire seasons calculated by decompose analysis at large-scale domain

	Weather effect	Fuel effect	Climate effect	Fix effect	Interaction effect
Spring-winter	12.57	21.39	33.23	22.93	10.87
Summer	16.26	17.29	35.79	21.8	8.87

Table S6. The mean variable importance metrics (%IncMSE) of each effect for the two fire seasons calculated based on grid burned area prediction

	Weather effect	Fuel effect	Climate effect	Fix effect
Spring-winter	8.20	9.04	12.09	6.56
Summer	9.12	4.85	19.18	4.59

Table S7. Comparison of MAE, MAE of large burned area, and standard deviation of predictions between the model with the chosen percentiles, percentile test 1, and percentile test set2

Model	**With the chosen percentiles***	**Percentile test set 1***	**Percentile test set 2***
MAE (log of area; winter-spring)	1.37	1.30	1.29
MAE of large burned area† (log of area; winter-spring)	2.13	2.64	2.81
Standard deviation of predictions (log of area; winter-spring)	2.42	2.09	2.09
MAE (log of area; summer)	1.17	1.12	1.11
MAE of large burned area† (log of area; summer)	2.25	2.42	2.52
Standard deviation of predictions (log of area; summer)	2.19	1.93	1.92

* Model developed in this study: Use the selected percentiles of 45, 55, 65, 85, 95, and 99 and six subgroups of (39, 49), (50, 59), (60, 69), (70, 79), (80, 89), (>=90).

* Set 1: Use the selected percentiles of 45, 55, 65, 75, 85, and 95 and six subgroups of (39, 49), (50, 59), (60, 69), (70, 79), (80, 89), (>=90).

* Set 2: Use the selected percentiles of 47.5, 63, 78, and 93 and four subgroups of (39, 55), (56, 70), (71, 85), (86, 100).

† Large burned area here is defined as the burned area larger than 90th percentile.

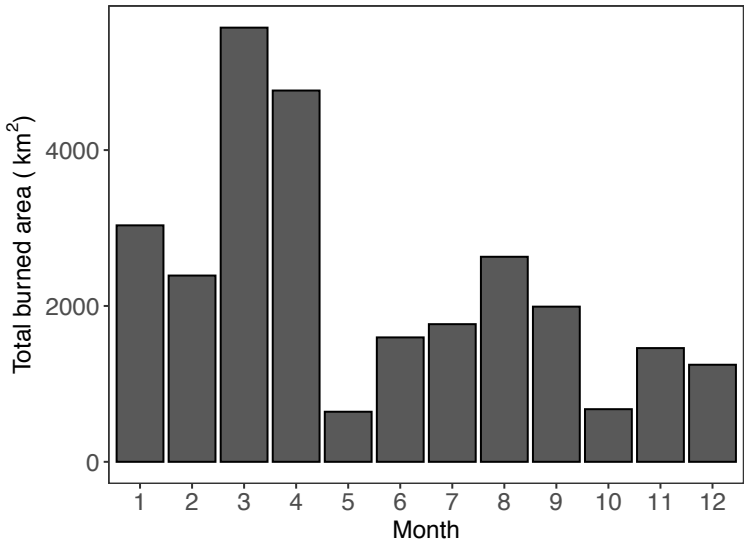

Figure S1. Seasonal burned area for the South Central US. It shows the monthly total burned area summed over 2002-2015.

60

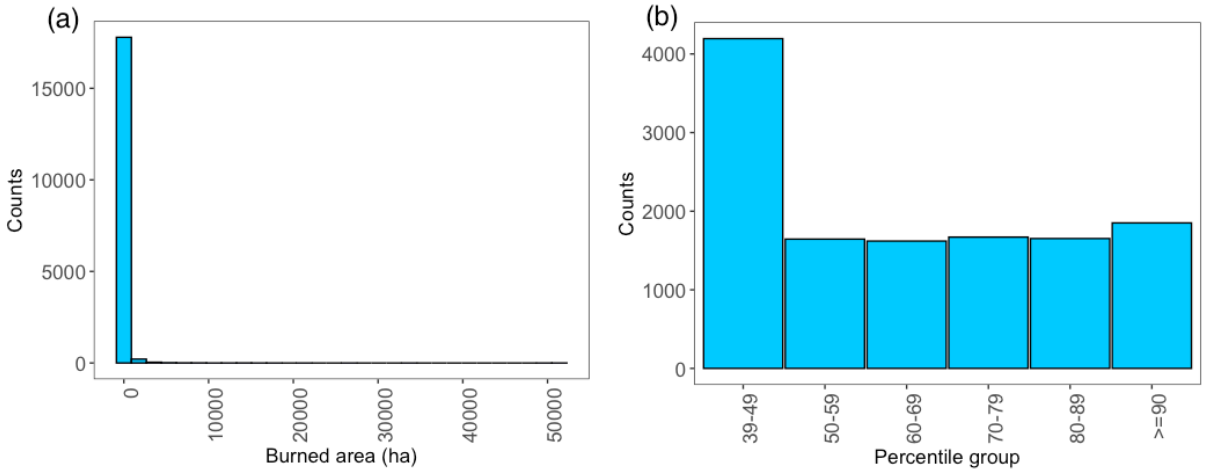

Figure S2. (a) Histogram of burned area of all the grids in winter-spring fire season and (b) histogram of the percentile groups of burned area for the winter-spring fire season.

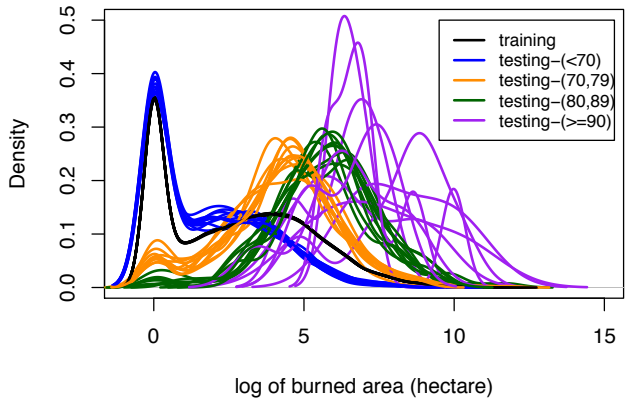

Figure S3. Probability distribution of burned area for 10 folds of the training set (black line), testing set predicted to have percentiles less than 70 (blue), between 70 and 79 (yellow), between 80 and 89 (green), and equal to or larger than 90 (purple).

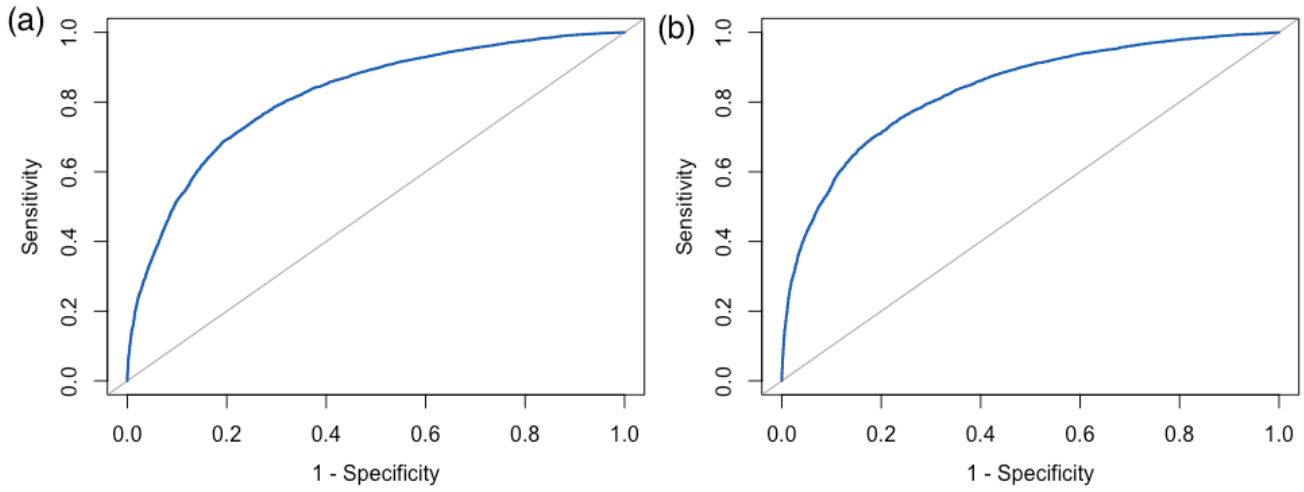

Figure S4. The ROC curve analysis of the logistic model for predicting burned grids in (a) winter-spring and (b) summer fire season.

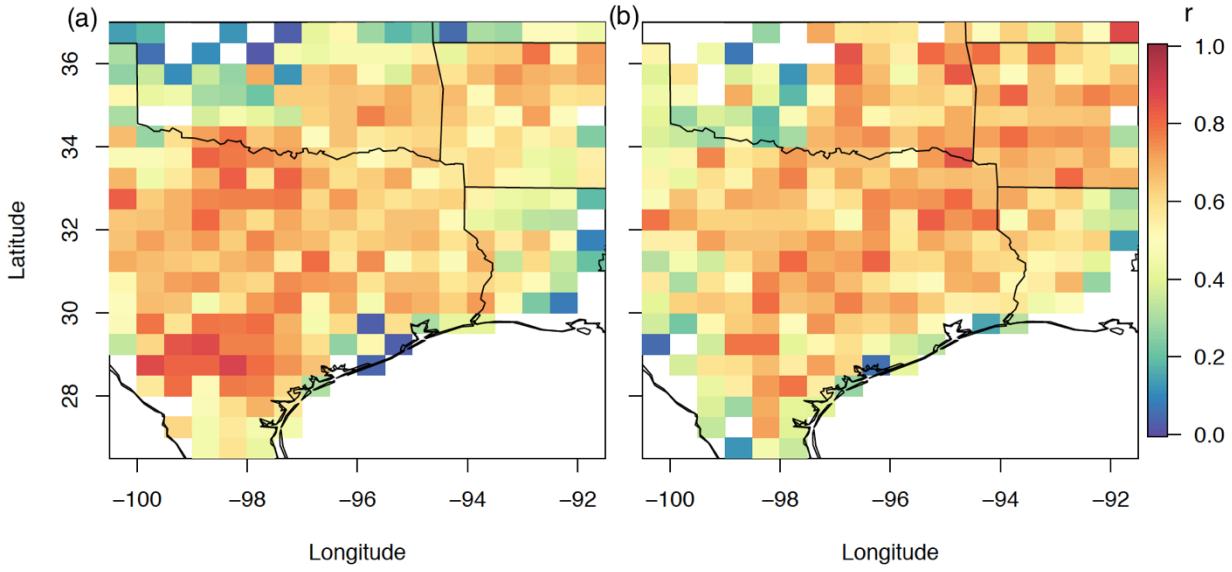

Figure S5. Maps of temporal correlation between observed and predicted burned area for each grid for the (a) winter-spring fire season (b) summer fire season.

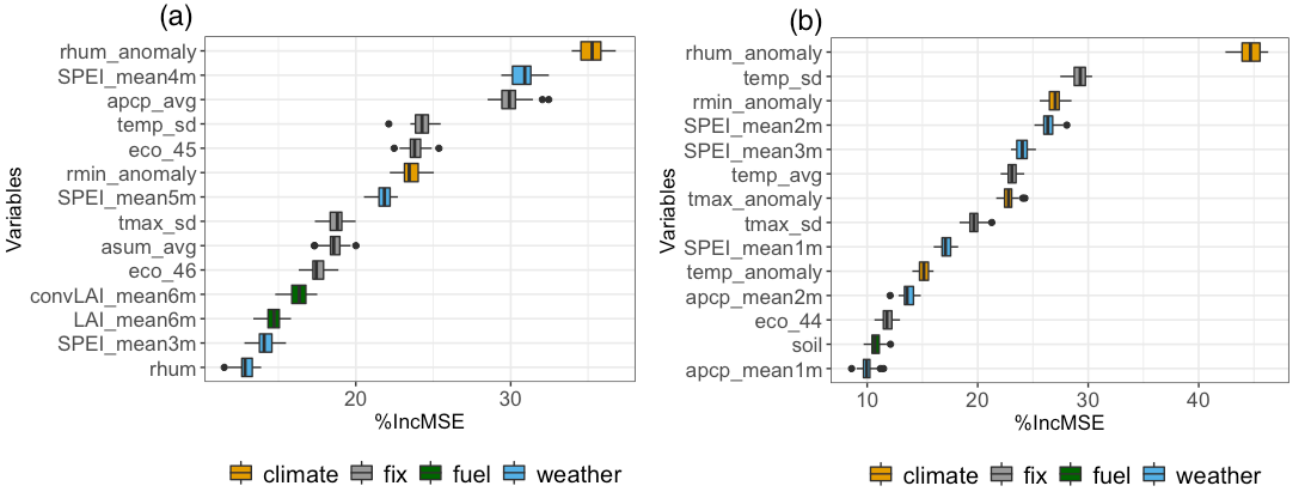

Figure S6. Box plots of variable importance in %IncMSE from the 50 times 10-fold cross validation for (a) winter-spring and (b) summer fire season.

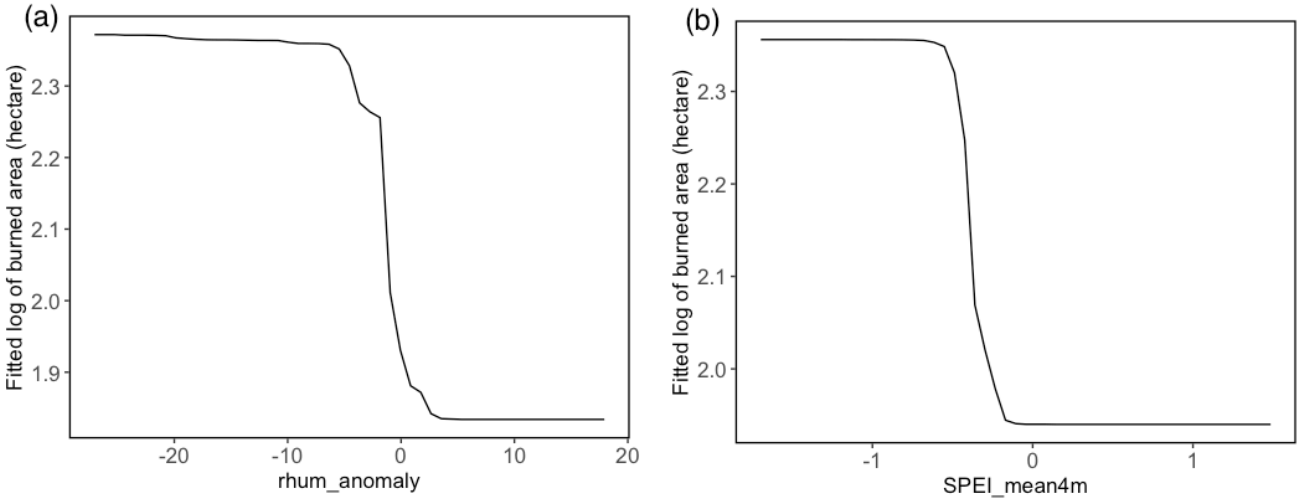

Figure S7. Partial dependence plots for the burned area model and (a) RH anomaly and (b) mean SPEI of the preceding 4 months for the winter-spring fire season.

90

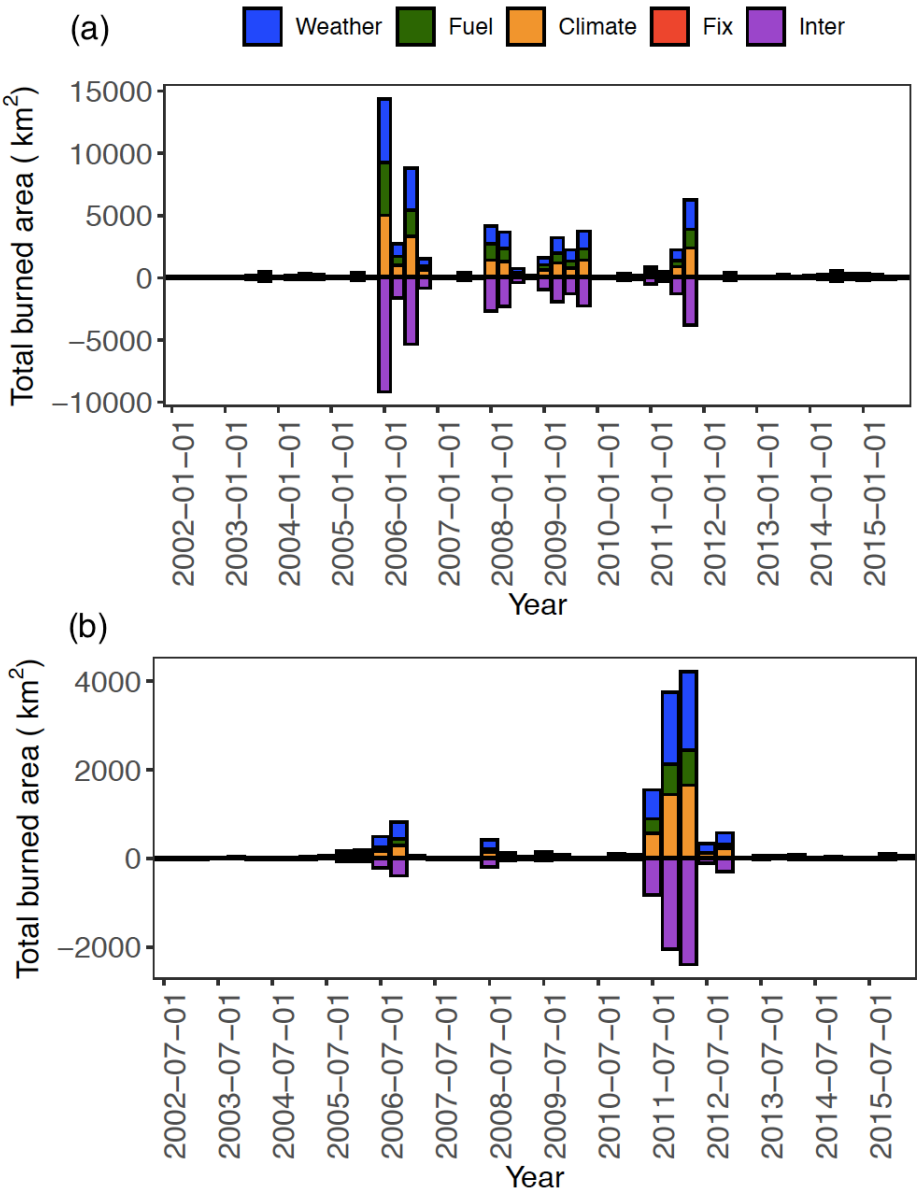

Figure S8. Timeseries of burned area contributed by different environmental controls for the (a) winter-spring and (b) summer fire season. Color of blue, green, yellow, red, and purple indicate effect of weather, fuel, climate, fix, and interaction.

95

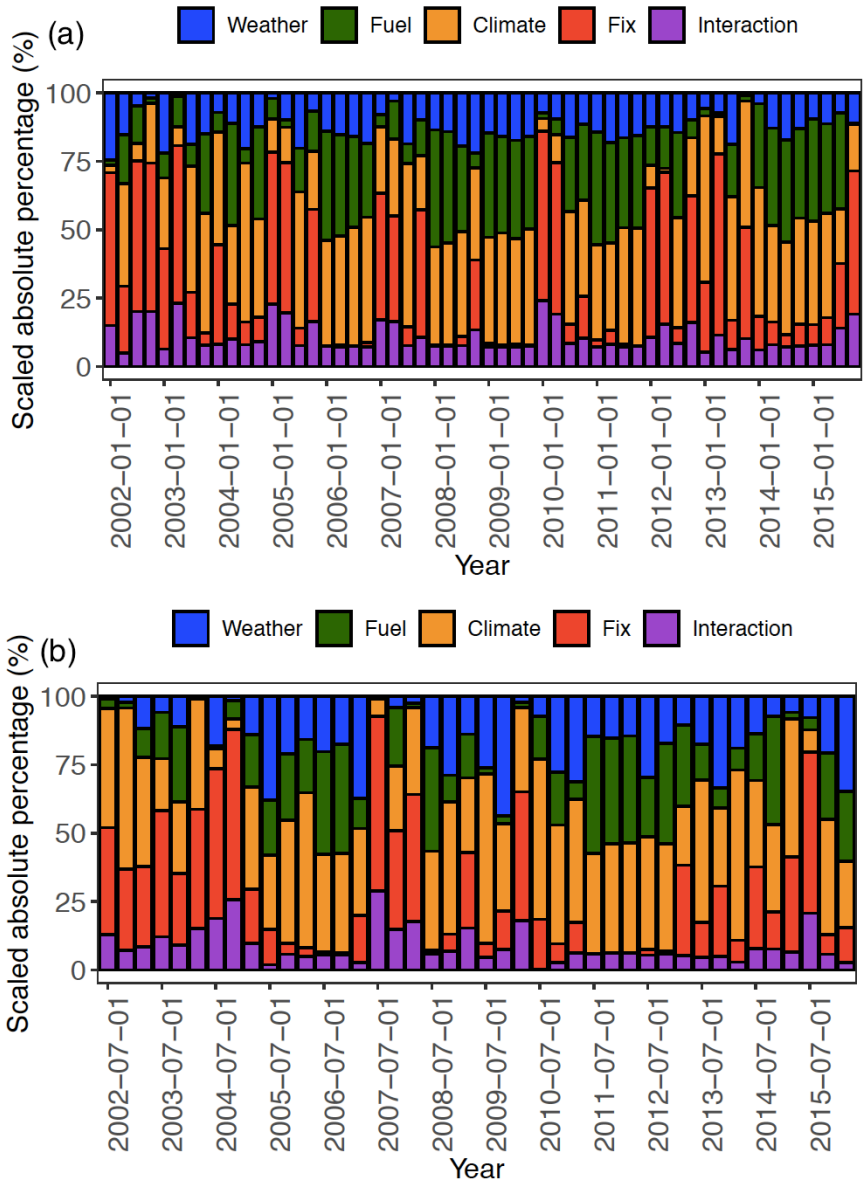

Figure S9. Timeseries of the scaled absolute percentage for the (a) winter-spring fire season and (b) summer fire season. Color of blue, green, yellow, red, and purple indicate effect of weather, fuel, climate, fix, and interaction.

100

Calculation of skewness

Skewness is a measure of the asymmetry of the probability distribution of a random variable about its mean. The skewness of a random variable X is the third standardized moment $\widetilde{\mu_3}$, defined as:

$$\widetilde{\mu_3} = E\left[\left(\frac{X-\mu}{\sigma}\right)^3\right] = \frac{\mu_3}{\sigma^3} = \frac{E[(X-\mu)^3]}{(E[(X-\mu)^2])^{3/2}} = \frac{\kappa_3}{\kappa_2^{3/2}} \quad (1)$$

where μ is the mean, σ is the standard deviation, E is the expectation operator, μ_3 is the third central moment, and κ_t are the *t*-th cumulants. If skewness is less than -1 or greater than +1, the distribution is highly skewed. If skewness is between -1 and -0.5 or between +0.5 and +1, the distribution is moderately skewed. If skewness is between -0.5 and 0.5, the distribution is approximately symmetric. The positive value indicates that the tail is on the right side of the distribution while negative value indicates that the tail is on the left.

Calculation of correlation coefficient (r)

We also calculated two types of correlation coefficient (r) to evaluate model performance: spatial r and temporal r. For the spatial r, for each month, we calculated the correlation coefficient of the prediction and observation for all the grids over the whole domain. As for the temporal r, for each grid, we calculated the correlation coefficient for the timeseries of observed and predicted burned area. At the end, we obtain a map showing the temporal R, demonstrated in Figure S5.

Method to decompose the relative influence of environmental controls

A set of sensitivity experiments was designed to decompose the effect of different environmental controls across our study domain by perturbing variables belonging to one category at a time. The environmental control categories to be perturbed include weather, climate, and fuel. The fix-geospatial factors remain unchanged in each sensitivity experiment. The variables of each category are listed in Table 1. First, to examine the influence of weather, for each grid, we assigned the values of individual weather variables to their 15-year means by grids while keeping the variation of other variables (hereafter refer to as the "weather-avg run"). The same procedure was applied to the variables in the climate and fuel category, resulting in the climate-avg run and fuel-avg run respectively. The original model with all the variables of each grid varying by time is called the full-model run. Second, the gridded burned area predicted from each run is summed over all the grids across the study domain. The differences in resulting total burned area between the full-model run and weather-avg run represent the impact of weather control (hereafter called "weather effect"), and the same procedure was applied to derive the climate effect and fuel effect on the burned area. We also conducted the fixed run, in which for each grid, its weather, climate anomaly, and fuel variables are all fixed to their long-term mean, and the predicted burned area from this run represents the influence of geospatial variables and climate normals on the burned area (hereafter named "fix effect"). Although the calculations of deriving the effect of a given environmental category are made by assuming linearity, the machine-learning-based prediction model does not assume linearity. Thus, the summation of burned area prediction from the weather, climate, fuel, and fixed run is not

necessarily equal to the burned area predicted by the full model. This difference is considered as the interaction effect among these environmental controls.

After deriving the effects of the environmental controls on the burned area, we then calculated such effects of environmental controls in the scaled absolute percentage. The effect of an environmental control category was normalized by the number of variables in that category because the numbers of variables are different by environmental control and the category with a larger number of variables may have a larger effect on the burned area. Then, the scaled absolute percentage is defined as the normalized absolute value of the effect of one environmental control divided by the summation of the normalized absolute values of all the effects over all the categories. Thus, the scaled absolute percentage represents the average effect of a single variable in each category. For example, Equation (1) shows how we calculated the scaled absolute percentage of the weather contribution on burned area:

$$\frac{|E_w|/N_w}{|E_w|/N_w + |E_{fu}|/N_{fu} + |E_c|/Nc + |E_{fi}|/N_{fi} + |E_i|/N_t}, \quad (2)$$

, where E is the influence of the environmental controls in burned area, N indicates the number of variables in the category, N_t is the total number of variables, and the subscript *w, fu, c, fi, and, i* represent weather, fuel, climate, fixed, and interaction, respectively.